Electronic Supplementary Material (ESI) for Catalysis Science & Technology.
This journal is © The Royal Society of Chemistry 2023

Supporting Information

Harnessing the Catalytic Plasticity of the *ent*-Kaurene Synthase from *Bradyrhizobium japonicum* to Produce the *ent*-Rosane and *ent*-Pimarane Scaffolds

Fan Zhang,[2,4†] Su-Jing Wang,[1,†] Wen Xiao,[1,†] Ming-Zhu Yu,[1] Feng Sha,[1] Ruibo Wu,*[2] Zheng Xiang*[1,3]

[1]State Key Laboratory of Chemical Oncogenomics, Guangdong Provincial Key Laboratory of Chemical Genomics, AI for Science (AI4S) Preferred Program, School of Chemical Biology and Biotechnology, Peking University Shenzhen Graduate School, Shenzhen 518055, China. [2]School of Pharmaceutical Sciences, Sun Yat-sen University, Guangzhou 510006, China. [3]Institute of Chemical Biology, Shenzhen Bay Laboratory, Shenzhen 518132, China. [4]Guangdong Provincial Key Laboratory of Translational Cancer Research of Chinese Medicines, International Institute for Translational Chinese Medicine, School of Pharmaceutical Sciences, Guangzhou University of Chinese Medicine, Guangzhou 510006, P. R. China.

Table of Contents

I. Supplementary schemes and figures

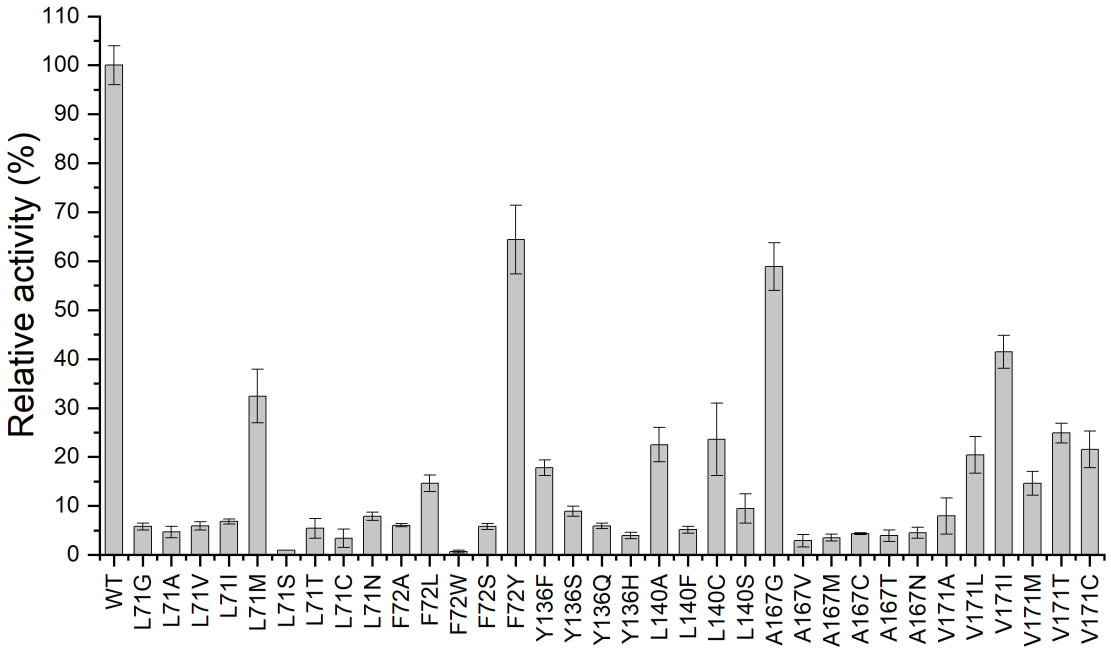

Figure S1. Catalytic activity of the BjKS variants relative to the wild-type BjKS.

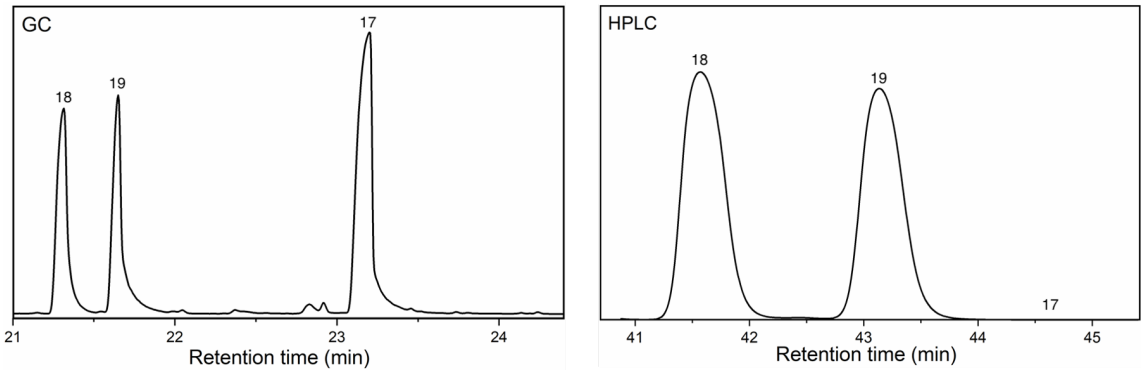

Figure S2. Chromatogram of GC-MS and HPLC analysis of the hydration products, i.e. compounds **17**, **18** and **19**.

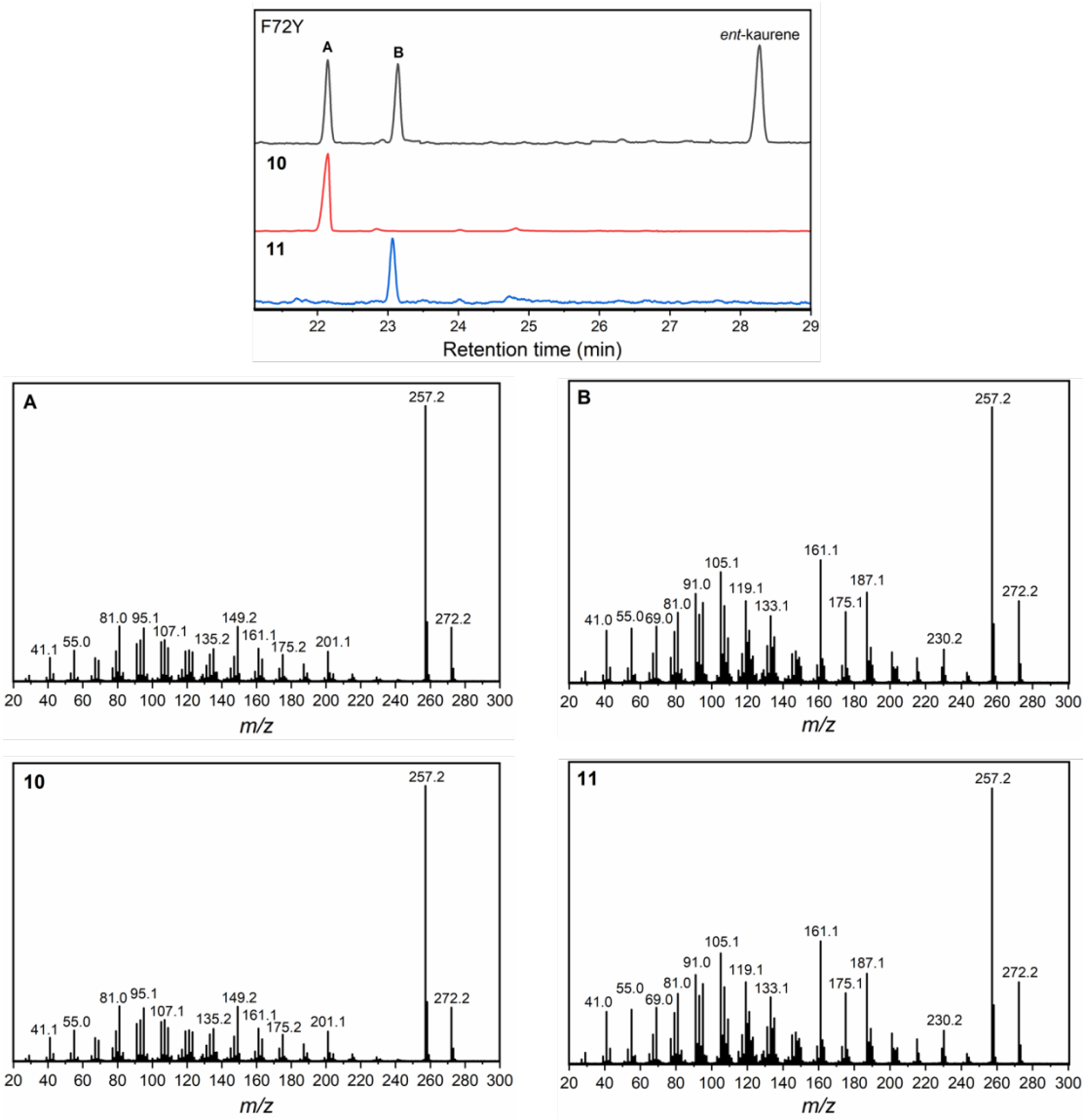

Figure S3. GC-MS analysis of compound **10**, compound **11** and comparing of metabolic products of BjKS-F72Y *in vivo* with the pure products of chemical transformation from metabolic products. Peak A: *ent*-rosa-5(10),15-diene (**10**); Peak B: *ent*-pimara-8(9),15-diene (**11**).

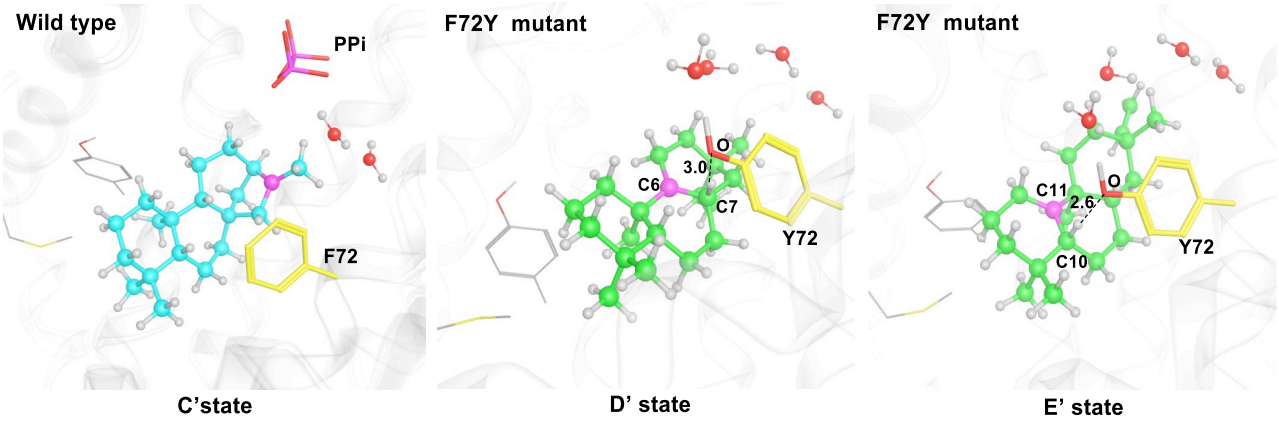

Figure S4. Representative structures for C' state in the wild-type BjKS and D'/E' state in the BjKS:F72Y mutant.

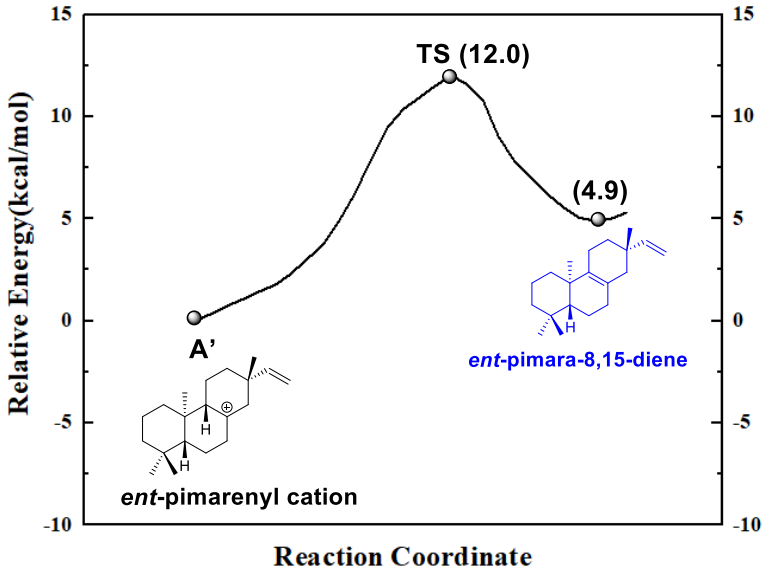

Figure S5. Relative energy profile of direct deprotonation from C6 of A' state to produce side product *ent*-pimara-8,15-diene (**11**).

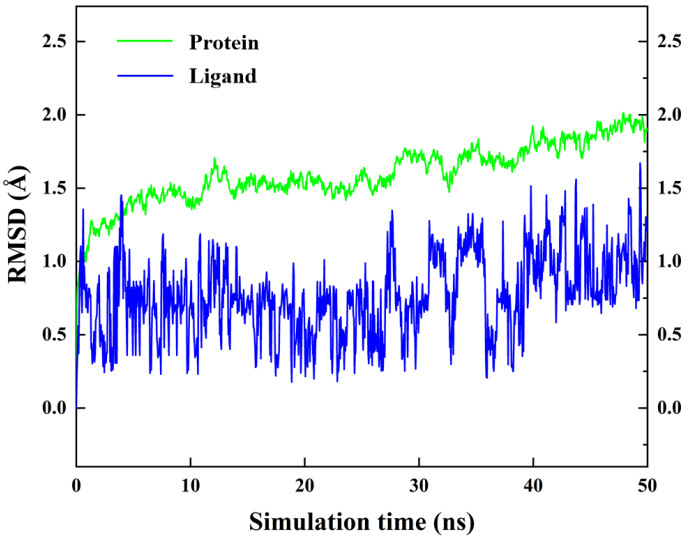

Figure S6. RMSD of wild type BjKS during the 50 ns MD simulations, the RMSD values become relatively stable in the last 10ns (40-50ns).

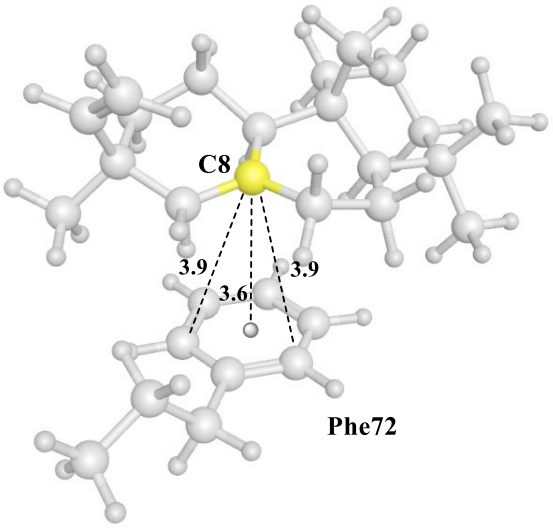

Figure S7. Binding energy of ent-primarenyl cation and ethylbenzene (representing Phe residue) calculated at M062X/6-31G(d). The distance is given in Å.

II. Materials and methods

Protein and codon-optimized nucleotide sequences

geranylgeranyl pyrophosphate synthase from *S. cerevisiae* (BTS1, 335 aa, 1008 bp)

MEAKIDELINNDPVWSSQNESLISKPYNHILLKPGKNFRLNLIVQINRVMNLPKDQLAIVSQIVELLHNSSLLIDDIEDNAPLRRGQT
TSHLIFGVPSTINTANYMYFRAMQLVSQLTTKEPLYHNLITIFNEELINLHRGQGLDIYWRDFLPEIIPTQEMYLNMVMNKTGGLFRL
TLRLMEALSPSSHHGHSLVPFINLLGIIYQIRDDYLNLKDFQMSSEKGFAEDITEGKLSFPIVHALNFTKTKGQTEQHNEILRILLLR
TSDKDIKLKLIQILEFDTNSLAYTKNFINQLVNMIKNDNENKYLPDLASHSDTATNLHDELLYIIDHLSEL

atggaggcgaagatcgacgaactgattaacaacgatccggtgtggagcagccagaacgagagcctgatcagcaaaccgtataaccaca
ttctgctgaagccgggtaaaaacttccgtctgaacctgatcgtgcaaattaaccgtgttatgaacctgccgaaggaccagctggcgat
cgtgagccaaattgttgagctgctgcacaacagcagcctgctgatcgacgatattgaagataacgcgccgctgcgtcgtggtcagacc
accagccacctgatcttcggcgtgccgagcaccattaacaccgcgaactacatgtattttcgtgcgatgcagctggttagccaactga
ccaccaaggaaccgctgtaccacaacctgatcaccattttcaacgaggaactgatcaacctgcaccgtggtcagggcctggacatcta
ctggcgtgattttctgccggagatcattccgacccaagaaatgtatctgaacatggtgatgaacaaaaccggtggcctgttccgtctg
accctgcgtctgatggaggcgctgagcccgagcagccaccacggtcacagcctggttccgtttatcaacctgctgggcatcatttacc
agattcgtgacgattatctgaacctgaaggacttccaaatgagcagcgaaaaaggttttgcggaggacatcaccgaaggcaaactgag
cttcccgattgtgcacgcgctgaactttaccaagaccaaaggccagaccgagcaacacaacgaaatcctgcgtattctgctgctgcgt
accagcgacaaggacatcaagctgaaactgatccagattctggagttcgacaccaacagcctggcgtacaccaaaaactttatcaacc
aactggttaacatgatcaagaacgataacgaaaacaagtatctgccggacctggcgagccacagcgataccgcgaccaacctgcacga
cgagctgctgtacatcattgatcacctgagcgaactgtaa

ent-copalyl diphosphate synthase from *Streptomyces platensis* (PtmT2, 533 aa, 1602 bp)

MLEVPAQPTPAPREAEAAALLAATVADPWGLVAPSVYDTARLVSLAPWLDGHRERLGYLAKEQNQDGSWGAPDGYGLVPTLSAVEALL
TELARTDSGAPHLSPDDLAAACADGLGALRDGLLAGPVPDTIGVEFVAPSLLADINTRLAALTEQAPGKLGAWSGTTLTSPAPDLDGA
LLAGVREMTEQAPLPEKLWHTLEAVTRDGTRGARPHEGAPPHNGSVGCSPAATAAWLGAAPDPAAPGVAYLRDVQARFGGPVPSITPI
VYFEQAWVLNSLAASGLRYEAPAALLDSLEAGLTDEGIAAAPGLPSDSDDTAAVLFALAQHGRTHRPDSLMHFRRDGYFSCFGVERTP
STSTNAHILEALGHHVTVRPDDAGRYGAEIRMISDWLLDNQLPDGSWMDKWHASPYYATACCALALAEFGGPSARAAVDRAAAWALAT
QRADGSWGRWQGTTEETAYMVQLLMRTRTPGSPGTVARSAARGCDALLAHDDPASYPGLWHDKDIYAPVTVIRAARLAALALGGAASA
ASGGA

atgctggaagttccggcccagccgaccccggcgccgcgtgaagcggaagcagcggcgctgctggccgctaccgtggctgatccgtggg
gtctggttgcgccgtccgtgtatgacaccgcgcgtctggtttctctggcgccgtggctggatggtcaccgtgaacgtctgggttacct
ggcgaaagaacagaatcaggatggctcttggggtgcaccggacggctacggcctggttccgaccctgagcgcggtggaagcgctgctg
accgaactggcgcgcaccgatagcggtgctccgcacctgtctccggatgatctggcggcagcgtgcgcggacggcctgggcgcgctgc
gtgacggcctgctggcaggcccggtgccggataccatcggcgttgaatttgttgcgccgtctctgctggcggacatcaacacccgtct
ggctgcactgaccgaacaggctccgggcaaactgggtgcttggtctggcaccaccttaaccagccctgctccggatctggacggtgcg
ctgctggcgggcgttcgtgaaatgaccgaacaggcgccgctgccagaaaaactgtggcacaccctggaagcggtaacccgtgatggca
cccgcggcgcccgtccgcacgaaggtgcaccgccgcacaacggctctgtcggctgctccccggcggcaaccgcggcgtggctgggtgc
cgcgccggacccggctgctccgggcgtggcatacctgcgcgatgtccaggcgcgtttcggtggtccggtgccgagcattaccccgatc
gtgtacttcgaacaggcatgggtgctgaacagcctggccgcatctggtctgcgttatgaggcgccggctgcactgctggatagcctgg
aagctggtctgaccgatgaaggcatcgcggcggcgccgggcctgccgtctgactccgatgataccgcggcggttctgttcgcgctggc
acaacacggtcgcacccaccgtccggatagcctgatgcacttccgccgtgacggctacttctcttgctttggcgttgaacgtaccccg

tccacctccaccaacgcgcacatcctggaagccctgggccaccacgttaccgtgcgtccggacgatgcgggtcgttacggcgcggaaa
tccgtatgatctctgattggcttctggataaccagttaccggatggctcctggatggacaaatggcacgcgtccccgtactacgcaac
cgcttgttgtgcgctggcgctggctgagttcggcggcccgtccgcccgcgcggcagtcgatcgtgctgcggcgtgggcgctggcaacc
cagcgtgcggatggtagctggggccgctggcagggcaccaccgaagaaaccgcctacatggttcagctgctgatgcgtacccgtactc
cgggctctccgggcaccgttgcgcgcagcgcggctcgtggttgcgacgcgctgctggcgcatgacgatccggcatcttatccgggttt
atggcatgataaagatatttatgcgccggttactgtgattcgtgcggcacgtttagcagcattagccttaggtggtgcagcaagcgca
gcatctggtggtgcgtaa

ent-kaurene synthase from _Bradyrhizobium japonicum_ (BjKS, 300 aa, 903 bp)

MIQTERAVQQVLEWGRSLTGFADEHAVEAVRGGQYILQRIHPSLRGTSARTGRDPQDETLIVTFYRELALLFWLDDCNDLGLISPEQL
AAVEQALGQGVPCALPGFEGCAVLRASLATLAYDRRDYAQLLDDTRCYSAALRAGHAQAVAAERWSYAEYLHNGIDSIAYANVFCCLS
LLWGLDMATLRARPAFRQVLRLISAIGRLQNDLHGCDKDRSAGEADNAVILLLQRYPAMPVVEFLNDELAGHTRMLHRVMAEERFPAP
WGPLIEAMAAIRVQYYRTSTSRYRSDAVRGGQRAPA

atgatccagaccgaacgtgcggttcagcaggttctggaatggggccgcagcctgaccggtttcgctgatgaacacgcggtggaagcgg
tgcgtggcggccagtacatcctccagcgtatccacccgtctctgcgtggcacctctgcgcgtacgggccgcgacccgcaggatgaaac
cctgattgttaccttctaccgcgaactggcgctgctgttctggctggatgactgcaacgacctgggtctgatctctccggaacagctg
gcggctgttgaacaggcgctgggccagggtgttccgtgcgcgctgccgggcttcgaaggttgcgcagttctgcgtgcgagcctggcga
ccctggcatacgaccgccgtgattacgcgcagctgctggacgacacccgttgctacagcgcggcgctgcgtgcgggccacgcgcaggc
tgttgcggcggaacgttggtcttacgctgaatacctgcacaacggtatcgattctatcgcgtacgcaaacgtgttctgctgtctgtcc
ctgctgtggggcctggatatggcgaccctgcgtgcgcgtccggcgttccgtcaggttctgcgtctgatctctgctattggccgtctgc
aaaacgacctgcacggttgcgacaaagatcgcagcgcgggtgaagcggataacgcggttatcctgctgttgcagcgttacccggcgat
gccggttgttgaatttctgaacgatgaactggcgggccacacccgtatgctgcatcgtgttatggctgaagaacgtttcccggcgccg
tggggtccgctgatcgaagcgatggcggcgatccgtgtgcagtactaccgcaccagcacctctcgttaccgtagcgatgcggttcgtg
gcggccagcgtgcgccggcgtaa

Site-directed mutagenesis

Site-directed mutagenesis was carried out using the overlap extension PCR with the primers described in **Table S1**. The resulting mutant genes were subcloned into pETDuet-BTS1-PtmT2 and verified by DNA sequencing.

Table S1. Primers used for site-directed mutagenesis of BjKS.

Primer	Nucleotide Sequence (5'-3')
BjKS-F	TCTGGTGGTGCGTAAGGATC
BjKS-R	GCCGATATCCAATTGAGATCTTTAC
BjKS-L71G-F	ACCGCGAACTGGCGCTGGGCTTCTGG
BjKS-L71G-R	CCAGAAGCCCAGCGCCAGTTCGCGGTAG
BjKS-L71A-F	ACCGCGAACTGGCGCTGGCGTTCTGG
BjKS-L71A-R	CCAGAACGCCAGCGCCAGTTCGCGGTAG
BjKS-L71V-F	ACCGCGAACTGGCGCTGGTGTTCTGG
BjKS-L71V-R	CCAGAACACCAGCGCCAGTTCGCGGTAG
BjKS-L71I-F	ACCGCGAACTGGCGCTGATCTTCTGG
BjKS-L71I-R	CCAGAAGATCAGCGCCAGTTCGCGGTAG

BjKS-L71M-F	ACCGCGAACTGGCGCTGATGTTCTGG
BjKS-L71M-R	CCAGAACATCAGCGCCAGTTCGCGGTAG
BjKS-L71S-F	ACCGCGAACTGGCGCTGAGCTTCTGG
BjKS-L71S-R	CCAGAAGCTCAGCGCCAGTTCGCGGTAG
BjKS-L71T-F	ACCGCGAACTGGCGCTGACCTTCTGG
BjKS-L71T-R	CCAGAAGGTCAGCGCCAGTTCGCGGTAG
BjKS-L71C-F	ACCGCGAACTGGCGCTGTGCTTCTGG
BjKS-L71C-R	CCAGAAGCACAGCGCCAGTTCGCGGTAG
BjKS-L71N-F	ACCGCGAACTGGCGCTGAACTTCTGG
BjKS-L71N-R	CCAGAAGTTCAGCGCCAGTTCGCGGTAG
BjKS-F72A-F	GAACTGGCGCTGCTGGCGTGGCTG
BjKS-F72A-R	CAGCCACGCCAGCAGCGCCAGTTC
BjKS-F72L-F	GAACTGGCGCTGCTGGTGTGGCTG
BjKS-F72L-R	CAGCCACACCAGCAGCGCCAGTTC
BjKS-F72W-F	GAACTGGCGCTGCTGTGGTGGCTG
BjKS-F72W-R	CAGCCACCACAGCAGCGCCAGTTC
BjKS-F72S-F	GAACTGGCGCTGCTGAGCTGGCTG
BjKS-F72S-R	CAGCCAGCTCAGCAGCGCCAGTTC
BjKS-F72Y-F	GAACTGGCGCTGCTGTATTGGCTG
BjKS-F72Y-R	CAGCCAATACAGCAGCGCCAGTTC
BjKS-Y136F-F	ACGACACCCGTTGCTTCAGC
BjKS-Y136F-R	GCTGAAGCAACGGGTGTCGTC
BjKS-Y136S-F	ACGACACCCGTTGCAGCAGC
BjKS-Y136S-R	GCTGCTGCAACGGGTGTCGTC
BjKS-Y136Q-F	ACGACACCCGTTGCCAGAGC
BjKS-Y136Q-R	GCTCTGGCAACGGGTGTCGTC
BjKS-Y136H-F	ACGACACCCGTTGCCATAGC
BjKS-Y136H-R	GCTATGGCAACGGGTGTCGTC
BjKS- L140A -F	GTTGCTACAGCGCGGCGGCGCGTG
BjKS- L140A -R	CACGCGCCGCCGCGCTGTAGCAAC
BjKS- L140F -F	GTTGCTACAGCGCGGCG TTTCGTG
BjKS- L140F -R	CACGAAACGCCGCGCTGTAGCAAC
BjKS- L140C -F	GTTGCTACAGCGCGGCGTGCCGTG
BjKS- L140C -R	CACGGCACGCCGCGCTGTAGCAAC
BjKS- L140S -F	GTTGCTACAGCGCGGCG AGC CGTG
BjKS- L140S -R	CACGGCTCGCCGCGCTGTAGCAAC
BjKS-A167G-F	GGTATCGATTCTATCGGCTACGC
BjKS-A167G-R	GCGTAGCCGATAGAATCGATACC
BjKS-A167V-F	GGTATCGATTCTATCGTGTACGC
BjKS-A167V-R	GCGTACACGATAGAATCGATACC
BjKS-A167M-F	ACGGTATCGATTCTATCATGTACGC
BjKS-A167M-R	GCGTACATGATAGAATCGATACCGTTG

BjKS-A167C-F	ACGGTATCGATTCTATCTGCTACGC
BjKS-A167C-R	GCGTAGCAGATAGAATCGATACCGTTG
BjKS-A167T-F	ACGGTATCGATTCTATCACCTACGC
BjKS-A167T-R	GCGTAGGTGATAGAATCGATACCGTTG
BjKS-A167N-F	GGTATCGATTCTATCAACTACGC
BjKS-A167N-R	GCGTAGTTGATAGAATCGATACC
BjKS-V171A-F	ATCGCGTACGCAAACGCGTTC
BjKS-V171A-R	GAACGCGTTTGCGTACGCGATAC
BjKS-V171L-F	ATCGCGTACGCAAACCTGTTC
BjKS-V171L-R	GAACAGGTTTGCGTACGCGATAC
BjKS-V171I-F	ATCGCGTACGCAAACATCTTC
BjKS-V171I-R	GAAGATGTTTGCGTACGCGATAC
BjKS-V171M-F	ATCGCGTACGCAAACATGTTCTG
BjKS-V171M-R	CAGAACATGTTTGCGTACGCGATAC
BjKS-V171C-F	ATCGCGTACGCAAACTGCTTCTG
BjKS-V171C-R	CAGAAGCAGTTTGCGTACGCGATAC
BjKS-V171T-F	ATCGCGTACGCAAACACCTTCTG
BjKS-V171T-R	CAGAAGGTGTTTGCGTACGCGATAC

Molecular cloning

The *PtmT2* and *BjKS* (wild-type) genes were amplified with pETDuet-BTS1-PtmT2-BjKS as template via PCR amplification with primers described in **Table S2** and cloned into pET28a(+) vector with NdeI/BamHI restriction site. The *F72Y* and *F72UAA* genes removing amber stop codon were amplified with primers described in **Table S2** and cloned into pLX(+) vector with NdeI/BglII restriction site to give pLX-BjKS-F72Y and pLX-BjKS-F72TAG fused with a C-terminal 6×His tag, respectively. The recombined plasmids were transformed into *E. coli* DH5α, and successful cloning was verified by DNA sequencing.

Table S2. Primers used for *in vitro* enzymatic assay.

Primer Name	Nucleotide Sequence (5'-3')
PtmT2-F	GTGCCGCGCGGCAGCCATATGCTGGAAGTTCCGGC
PtmT2-R	ACGGAGCTCGAATTCGGATCCTTACGCACCACCAG
BjKS-WT-F	GTGCCGCGCGGCAGCCATATGATCCAGACCGAACGTGCG
BjKS-WT-R	ACGGAGCTCGAATTCGGATCCTTACGCCGGCGCACGCTG
BjKS-F72Y-F	GAACTGGCGCTGCTGTACTGGCTGGATG
BjKS-F72Y-R	CAGTACAGCAGCGCCAGTTCGCGGTAGAAG
BjKS-F72UAA-F	GAACTGGCGCTGCTGTAGTGGCTGGATG
BjKS-F72UAA-R	CACTACAGCAGCGCCAGTTCGCGGTAGAAG

pLX-NdeI -F	CATTAAAGAGGAGAAATTCATATGATCCAGACCGAACGTGC
pLX-BglII -R	ATGGTGATGGTGATGAGATCTCGCCGGCGCACGCTGGCCG

III. Experimental procedures for chemical transformation

General information

All the reactions were carried out under an argon atmosphere with dry solvents. Reagents were used without further purification. Solvent purification was conducted according to *Purification of Laboratory Chemicals* (Peerrin, D. D.; Armarego, W. L. and Perrins, D. R., Pergamon Press: Oxford, 1980). Reactions were monitored by thin-layer chromatography (TLC) carried out on 0.25 mm Tsingdao silica gel plates (GF-254). Staining was performed with an ethanolic solution of phosphomolybdic acid (PMA), or by oxidative staining with an aqueous basic potassium permanganate ($KMnO_4$) solution and subsequent heating. Tsingdao silica gel (60, particle size 0.040-0.063 mm) was used for flash column chromatography. NMR spectra were recorded on Brüker Advance 500 (^{1}H: 500 MHz, ^{13}C: 126 MHz). Residual undeuterated solvent was used as an internal reference ($CDCl_3$: ^{1}H NMR δ_H = 7.26 ppm, ^{13}C NMR δ_C = 77.16 ppm). The following abbreviations were used to explain the multiplicities: s = singlet, d = doublet, t = triplet, q = quartet, m = multiplet, br = broad. High-resolution mass spectra (HRMS) were measured on Thermo Q Exactive Focus. The ionization method is ESI and the mass analyzer type of TOF. IR spectra were recorded on an IR Prestige-21 FTIR spectrometer with a KBr disc. Optical rotation values were recorded on a Rudolph Research Analytical Autopol I polarimeter (Rudolph Research Co.).

Experimental procedures and spectral data

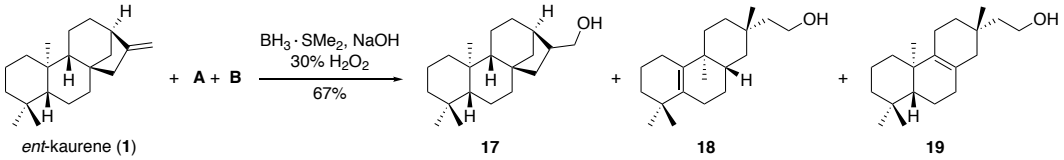

ent-kaurene (**1**) **17** **18** **19**

To the mixture of *ent*-kaurene, compound A, and compound B (98 mg, 0.36 mmol) in THF (3 mL) at 0 °C was added $BH_3 \cdot SMe_2$ (2 M in THF, 0.36 mL, 0.72 mmol) dropwise[1]. The reaction mixture was stirred at room temperature for 8 h, after which the solution was cooled to 0 °C and treated with methanol slowly. After stirring for 0.5 h, the mixture was concentrated under reduced pressure and the residue was dissolved in THF. Aqueous NaOH (3 M, 4 mL, 12 mmol) and aqueous hydrogen peroxide (30%, 4 mL) were added to the solution. After stirring at room temperature for 8 h, the reaction mixture was extracted with ethyl acetate and the organic phase was washed

with saturated aqueous $Na_2S_2O_3$, brine, dried over Na_2SO_4, and filtered. The filtrate was concentrated under reduced pressure. The residue was purified by flash chromatography (silica gel, ethyl acetate/hexane = 1/19 to 1/9) to give the mixture of compound **17**, **18** and **19** (71 mg, 0.24 mmol, 67%). TLC: R_f = 0.4 (silica gel, ethyl acetate/hexane = 1/9).

The mixture of compound **17**, **18** and **19** was dissolved in methanol, and separated by using semi-preparative HPLC on Shimadzu LC-20A with an Agilent ZORBAX Eclipse XDB-C18 column (9.4 × 250 mm, 5 μm particle size). The semi-preparative HPLC was performed with a 49 min gradient elution using solvent A (water) and solvent B (methanol) with a flow rate of 1 mL/min. The gradient elution is as follows: 0-2 min, 20% methanol; 2-15 min, a linear gradient of methanol from 20% to100%; 15–45 min, 100% methanol; 45–46 min, a linear gradient of methanol from 100 to 20%; 46–49 min, 20% methanol. The elution process was monitored by absorbance at a wavelength 200 nm (**Figure S3**). The fractions of each compound were collected and concentrated under reduced pressure to give compound **17** (18.0 mg, no absorbance), compound **18** (13.0 mg) and compound **19** (9.0 mg).

Compound **18**: colorless needle. $[\alpha]_D^{26.3}$ = +47.88 (*c* 0.52, $CHCl_3$). **^{1}H NMR** (500 MHz, $CDCl_3$) δ 3.74 (m, 2H), 2.02 (m, 2H), 1.88 (m, 2H), 1.59 (m, 2H), 1.51 (d, *J* = 3.3 Hz, 2H), 1.46 (m, 2H), 1.41 (m, 2H), 1.33 (m, 2H), 1.28 (d, *J* = 6.1 Hz, 2H), 1.23 (dd, *J* = 6.1, 3.0 Hz, 2H), 1.05 (m, 1H), 0.96 (s, 3H), 0.95 (s, 3H), 0.95 (s, 3H), 0.82 (s, 3H). **^{13}C NMR** (126 MHz, $CDCl_3$) δ 136.56, 133.29, 59.58, 49.14, 41.14, 39.95, 37.81, 37.54, 34.06, 32.75, 31.83, 29.12, 27.94, 26.08, 25.45, 25.33, 23.58, 20.00, 17.15. **IR** (KBr, cm^{-1}) 3615, 3312, 2964, 2921, 2868, 2846, 2358, 2342, 2330, 1469, 1452, 1433, 1380, 1359, 1262, 1045, 1028, 988. **HRMS-ESI** (*m/z*): $[M + H]^+$ calcd for $C_{20}H_{35}O$, 291.2688; found, 291.2682.

Comparison of NMR data for compound 18 to literature values ($CDCl_3$; δ, ppm)[2]

^{1}H NMR ($CDCl_3$)			^{13}C NMR ($CDCl_3$)		
Synthetic δ_H (ppm)	Literature δ_H (ppm)	Δδ (ppm)	Synthetic δ_C (ppm)	Literature δ_C (ppm)	Δδ (ppm)
3.74 (m, 2H)	3.73 (t, 8, 2H)	0.01	136.56	136.60	-0.04
2.02 (m, 2H)	0.8-2.1 (m, 19H)	/	133.29	133.32	-0.03
1.95–1.85 (m, 2H)			59.58	59.50	0.08
1.59 (m, 2H)			49.14	49.15	-0.01
1.51 (d, 3.3, 2H)			41.14	41.15	-0.01
1.46 (m, 2H)			39.95	39.99	-0.04
1.41 (m, 2H)			37.81	37.83	-0.02
1.33 (m, 2H)			37.54	37.70	-0.16

1.28 (d, 6.1, 2H)			34.06	34.04	0.02
1.23 (dd, 6.1, 3.0, 2H)			32.75	32.72	0.03
1.05 (m, 1H)			31.83	31.88	-0.05
0.96 (s, 3H)	0.97 (s, 3H)	-0.01	29.12	29.06	0.06
0.95 (s, 3H)	0.95 (s, 3H)	0.00	27.94	27.90	0.04
0.95 (s, 3H)	0.94 (s, 3H)	0.01	26.08	26.08	0.00
0.82 (s, 3H)	0.82 (s, 3H)	0.00	25.45	25.40	0.05
			25.33	25.27	0.06
			23.58	23.56	0.02
			20.00	19.97	0.03
			17.15	17.09	0.06

Compound **19**: colorless oil. $[\alpha]_D^{27.0}$ = -32.91 (*c* 0.55, $CHCl_3$).**^{1}H NMR** (500 MHz, $CDCl_3$) δ 3.81–3.70 (m, 1H), 1.95–1.86 (m, 2H), 1.74 (dd, *J* = 19.7, 8.4 Hz, 1H), 1.68–1.56 (m, 1H), 1.53–1.48 (m, 2H), 1.46–1.37 (m, 2H), 1.28–1.24 (m, 2H), 1.14 (dt, *J* = 12.5, 6.1 Hz, 1H), 1.02 (td, *J* = 13.0, 3.6 Hz, 1H), 0.95 (s, 2H), 0.88 (s, 2H), 0.84 (s, 3H). **^{13}C NMR** (126 MHz, $CDCl_3$) δ 136.82, 124.33, 77.41, 52.00, 46.34, 43.54, 41.99, 37.67, 36.81, 34.89, 33.44, 33.38, 32.85, 30.79, 23.19, 21.82, 20.73, 19.56, 19.16, 19.08. **IR** (KBr, cm^{-1}) 2954, 2924, 2854, 2359, 2307, 1749, 1459, 1377, 1261, 1146, 1024, 962. 808. **HRMS-ESI** (*m/z*): $[M + H]^+$ calcd for $C_{20}H_{35}O$, 291.2688; found, 291.2682.

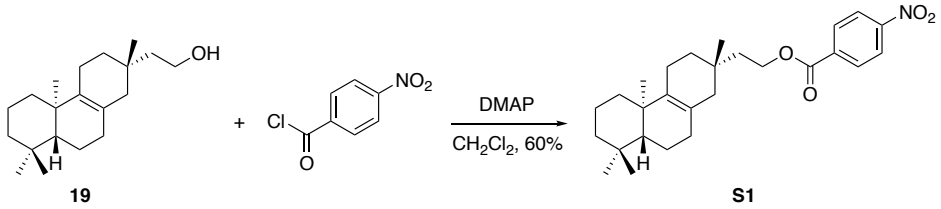

To a solution of compound **19** (8.0 mg, 0.028 mmol) in dichloromethane (1 mL) was added 4-(dimethylamino)-pyridine (10.3 mg, 0.084 mmol) and 4-nitrobenzoylchloride (12.8 mg, 0.069 mmol).[3] This reaction mixture was allowed to stir at room temperature for 24 h. Saturated aqueous $NaHCO_3$ (3 mL) was added to the reaction mixture, and the aqueous layer was extracted with dichloromethane (3 × 3 mL). The combined organic phase was washed with brine, dried over anhydrous Na_2SO_4, and concentrated under reduced pressure. The residue was purified by flash column chromatography (ethyl acetate/hexane = 1/50 to 1/20) to give compound **S1** (7.5 mg, 0.017 mmol, 60%) as a white solid. TLC: R_f = 0.60 (silica gel, ethyl acetate/hexane = 1/15). Solvent for growing crystal: acetone, ethanol and acetonitrile (1/1/1, v/v/v). $[\alpha]_D^{25.3}$ = -19.71 (*c* 0.36, $CHCl_3$). **^{1}H NMR** (500 MHz, $CDCl_3$) δ 8.30–8.27

(m, 2H), 8.22–8.18 (m, 2H), 4.49–4.43 (m, 2H), 1.97 (m, 2H), 1.88 (m, 2H), 1.85–1.75 (m, 2H), 1.74–1.70 (m, 2H), 1.59 (dd, J = 10.2, 6.6 Hz, 4H), 1.49–1.38 (m, 4H), 1.31 (ddd, J = 33.4, 19.5, 11.7 Hz, 2H), 1.18–1.12 (m, 2H), 1.04 (dd, J = 13.4, 9.7 Hz, 1H), 0.97 (s, 3H), 0.92 (s, 3H), 0.88 (s, 3H), 0.84 (s, 3H). **^{13}C NMR** (126 MHz, $CDCl_3$) δ 164.95, 150.67, 136.98, 136.09, 130.79, 124.14, 123.67, 63.36, 52.02, 43.45, 42.00, 41.48, 37.72, 36.85, 34.77, 33.46, 33.39, 32.87, 30.94, 23.17, 21.83, 20.74, 19.61, 19.17, 19.08. **IR** (KBr, cm^{-1}) 2959, 2923, 2849, 2828, 2365, 2344, 2317, 1716, 1528, 1459, 1349, 1319, 1273, 1101, 872, 800, 751, 718. **HRMS-ESI** (*m/z*): $[M + H]^+$ calcd for $C_{27}H_{38}NO_4$, 440.2795; found, 440.2763.

Crystallographic data of S1

CCDC 2042524 contains the supplementary crystallographic data for compound **S1**. These data can be obtained free of charge from the Cambridge Crystallographic Data Centre via www.ccdc.cam.ac.uk/data_request/cif.

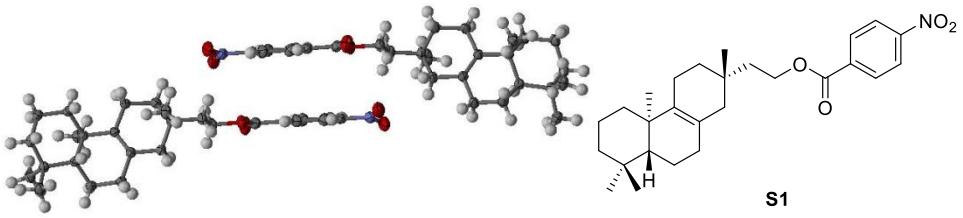

To a solution of compound **18** (7.6 mg, 0.026 mmol) and 2-NO_2PhSeCN (17.8 mg, 0.078 mmol) in THF (0.5 mL) was added *n*-Bu_3P (19.5 μL, 0.078 mmol) slowly, at which point the reaction mixture became deep red in color.[4] This solution was allowed to stir at 23 °C for 7 h, after which compound **18** has been completely consumed. The reaction mixture was cooled to 0 °C and aqueous hydrogen peroxide (30% w/w, 91 μL) was added cautiously. This orange solution was then stirred while gradually warming to 23 °C over c.a. 2 h and then stirred at 23 °C for additional 18 h. The reaction was then loaded directly onto a column and purified by flash chromatography (hexanes) to afford compound **10** (2.5 mg, 0.009 mmol, 40%) as a colorless oil. TLC: R_f = 0.96 (silica gel, hexane). Compound **10** has the same retention time and mass spectrum with peak **A** by GC-MS analysis (**Figure S4**). $[\alpha]_D^{25.7}$ = 43.67 (*c* 0.3, $CHCl_3$). **^{1}H NMR** (500 MHz, $CDCl_3$) δ 5.83 (dd, J = 17.5, 10.7 Hz, 1H), 4.92 (dd, J = 17.5, 1.4 Hz, 1H), 4.84 (dd, J = 10.7, 1.4 Hz, 1H), 2.13–1.86 (m, 4H), 1.63–1.57 (m, 2H), 1.54–1.23 (m, 12H), 1.03 (s, 3H), 0.98 (s, 3H),

0.97 (s, 2H), 0.84 (s, 4H). **^{13}C NMR** (126 MHz, $CDCl_3$) δ 151.68, 136.60, 133.32, 108.65, 39.98, 39.92, 37.85, 37.43, 36.58, 34.09, 32.85, 31.84, 29.14, 27.96, 26.05, 25.47, 25.34, 23.25, 20.02, 17.18. **IR** (KBr, cm^{-1}) 3082, 2954, 2924, 2854, 2390, 2285, 1640, 1581, 1474, 1459, 1376, 1359, 1261, 1018, 998, 907. **HRMS-ESI** (*m/z*): $[M + H]^+$ calcd for $C_{20}H_{33}$, 273.2577; found, 273.2578.

Comparison of NMR data for compound 10 to literature values ($CDCl_3$; δ, ppm)[2]

^{1}H NMR ($CDCl_3$)			^{13}C NMR ($CDCl_3$)		
Synthetic δ_H (ppm)	Literature δ_H (ppm)	Δδ (ppm)	Synthetic δ_C (ppm)	Literature δ_C (ppm)	Δδ (ppm)
5.83 (dd, 17.5, 10.7, 1H)	5.84 (dd, 16.9, 10.7, 1H)	-0.01	151.68	151.57	0.11
4.92 (dd, 17.5, 1.4, 1H)	4.93 (dd, 16.9, 1.5, 1H)	-0.01	136.60	136.55	0.05
4.84 (dd, 10.7, 1.4, 1H)	4.86 (dd, 10.7, 1.5, 1H)	-0.02	133.32	133.26	0.06
2.13–1.86 (m, 4H)	1.8–2.2 (m, 4H)		108.65	108.64	0.01
1.63–1.57 (m, 2H)	1.2–1.7 (m, 13H)	/	39.98	39.93	0.05
1.54–1.23 (m, 11H)			39.92	39.88	0.04
1.03 (s, 3H)	1.05 (s, 3H)	-0.02	37.85	37.80	0.05
0.98 (s, 3H)	1.00 (s, 3H)	-0.02	37.43	37.38	0.05
0.97 (s, 3H)	0.98 (s, 3H)	-0.01	36.58	36.51	0.07
0.84 (s, 3H)	0.86 (s, 3H)	-0.02	34.09	34.04	0.05
			32.85	32.81	0.04
			31.84	31.81	0.03
			29.14	29.12	0.02
			27.96	27.93	0.03
			26.05	26.01	0.04
			25.46	25.44	0.02
			25.34	25.30	0.04
			23.25	23.21	0.04
			20.02	19.98	0.04
			17.18	17.15	0.03

Compound **19** was converted into compound **11** with the same procedure. Unfortunately obtain the NMR spectra of compound **11** were not obtained due to trace amount of compound **11**. Compound **11** has the same retention time and mass spectrum with peak **B** by GC–MS analysis (**Figure S4**) **HRMS-ESI (m/z):** $[M + H]^+$ calcd for $C_{20}H_{33}$, 273.2577; found, 273.2578.

IV. Computational details

System setup

Although many crystal structures of BjKS have been solved to date, there is no crystal structure reported with

substrate or intermediate analogues in the active site. Thus, we had to reconstruct a reliable BjKS model with key intermediate binding and intact coordination shell. The crystal structure (PDB entry: 4W4S) with BPH-629 binding in active site was adopted (using one chain of the dimer) as the original model. Based on class I terpene synthases with the existence of similar Mg^{2+} ions coordination shell (such as ATAS and FSTS),[5, 6] the Mg^{2+} coordination shell (including PPi group and three Mg^{2+} ions) was rebuilt by superimposing the crystal structures of ATAS (PDB:4KUX) onto BjKS. Restrained MD simulations were performed to ensure the conserved coordination residues forming coordination with Mg^{2+} ions, and the coordinated water molecules could be replenished during MD simulations. According to the proposed reaction pathways and product spectrum of F72Y BjKS mutant, intermediate *ent*-pimarenyl cation was used as our starting point for system setup and subsequent computational studies. The intermediate was docked into BjKS using Glide SP mode (Schrödinger, LLC, New York)[7] with flexible sampling for ligand, and the orientation of intermediate could be speculated and selected according to the structure of original substrate *ent*-CPP. The protonation state of the protein residues was evaluated using H++.[8] The obtained enzyme-ligand complex model was used for further MD simulations to relax the structure of protein and intermediate conformations.

Classical MD Simulations

The Amber ff99SB force field[9] was employed for the protein and the TIP3P model was used for water molecules[10]. The force field parameters of the ligand were generated from the general AMBER force field (GAFF)[11], and the partial atomic charge of substrates was defined by the restrained electrostatic potential (RESP)[12] charge from the HF/6-31G* calculation with the Gaussian 09 package.[13] The initial coordinates and topology files were generated by the *tleap* program in AMBER12.[14] The MD simulations were carried out using the AMBER12 molecular simulation package, and the periodic boundary condition with cubic models were employed. For the routine minimization, three minimizations steps were performed, first by constraining all solute atoms then the protein backbone and finally no constraint. Each minimization step with 5000 cycles of steepest descent and 5000 cycles conjugate gradient. After minimization, each system was gradually heated from 0 to 300 K under the NVT ensemble for 100 ps (with Langevin thermostat), followed by another 100 ps NPT ensemble MD simulations at 300 K and the target pressure of 1.0 atm (with Berendsen barostat). Afterward, 50 ns NVT production MD simulations with a target temperature of 300 K were performed to produce trajectories. An RMSD analysis was performed to evaluate the stability of the system (Figure S6). The F72Y mutant was built based on the initial structure, similar MD protocols were used for wild type and F72Y mutant. During the MD simulations, the SHAKE algorithm[15] was

applied to constrain the high-frequency stretching vibration of all hydrogen-containing bonds, and a cutoff of 12 Å was set for both vdW (LJ-12 potential) and electrostatic interactions (PME strategy). Finally, snapshots of each system from the stable trajectories were chose to build the initial structures for the subsequent QM/MM simulations.

QM/MM MD Simulations

The periodic boundary condition was also considered in the following QM/MM MD simulations. The F72/Y72 together with the *ent*-pimarenyl cation were included in the QM region of wildtype and mutant BjKS models. There are 68 QM atoms for wild type BjKS and 70 QM atoms for the F72Y mutant (40989 atoms for the whole system including solvent), the charge of QM region is 1. All of these QM atoms were described with the M06-2X[16, 17]/6-31G(d) basis set which is widely used in studying cyclization reaction,[18, 19] and the model contains about 500 basis functions in total. The QM/MM boundary was treated by the improved pseudo bond approach.[20-22] The same force field in the aforementioned classical MD simulations was used for the remaining atoms. The 12 Å cutoff was employed for both van der Waals interaction by 12-6 Lennard-Jones potential function and electrostatic interactions by dual-focal ai-QM/MM-PME approach.[23] The QM/MM systems were minimized again for several iterations and more than 20 ps QM/MM MD simulations were performed. The resulting conformations of QM/MM MD (at least three from different time periods, 10/15/20ps) were used to map out the minimum energy path (MEP) using the reaction coordinate driving method[24]. After mapping out the MEP, the MM sub-system were further equilibrated by 500 ps free energy perturbation (FEP) simulations, with QM sub-system fixed at previously QM/MM minimized structures. Finally, the resulting snapshots were treated as the starting structures for QM/MM MD umbrella sampling[25]. Each window was calculated for at least 20 ps with 1 fs time step. The overlap of histogram between neighboring windows will be checked to confirm if each window were adequately sampled along the proper reaction coordinate, and then WHAM[26, 27] program was employed to calculate the free energy profile. The convergence of QM/MM MD umbrella sampling can be estimated by the free energy profile gap calculated from different time spans. All of these QM/MM calculations were performed with the interfaced QChem[28]-AMBER12 programs.[23]

Reference

1. Clay, J. M.; Vedejs, E., Hydroboration with pyridine borane at room temperature. *Journal of the American Chemical Society* **2005,** *127* (16), 5766-7.

2. Moiseenkov, A. M.; Dragan, V. A.; Veselovskii, V. V.; Shashkov, A. S., Syhthesis of Rosane diterpenes *Bulletin of the Academy of Sciences of the Ussr Division of Chemical Science* **1991,** *40* (8), 1682-1691.

3. Zhu, W.; Fang, J.; Liu, Y.; Ren, J.; Wang, Z., Lewis Acid Catalyzed Formal Intramolecular [3+2] Cross-Cycloaddition of Cyclopropane 1,1-Diesters with Alkenes: General and Efficient Strategy for Construction of

Bridged [n.2.1] Carbocyclic Skeletons. *Angewandte Chemie International Edition* **2013,** *52* (7), 2032-2037.
4. Hafeman, N. J.; Loskot, S. A.; Reimann, C. E.; Pritchett, B. P.; Virgil, S. C.; Stoltz, B. M., The Total Synthesis of (−)-Scabrolide A. *Journal of the American Chemical Society* **2020,** *142* (19), 8585-8590.
5. Chen, M.; Al-lami, N.; Janvier, M.; D'Antonio, E. L.; Faraldos, J. A.; Cane, D. E.; Allemann, R. K.; Christianson, D. W., Mechanistic insights from the binding of substrate and carbocation intermediate analogues to aristolochene synthase. *Biochemistry* **2013,** *52* (32), 5441-5453.
6. Zhang, F.; An, T.; Tang, X.; Zi, J.; Luo, H.-B.; Wu, R., Enzyme Promiscuity versus Fidelity in Two Sesquiterpene Cyclases (TEAS versus ATAS). *ACS Catal.* **2020,** *10* (2), 1470-1484.
7. Friesner, R. A.; Murphy, R. B.; Repasky, M. P.; Frye, L. L.; Greenwood, J. R.; Halgren, T. A.; Sanschagrin, P. C.; Mainz, D. T., Extra Precision Glide:? Docking and Scoring Incorporating a Model of Hydrophobic Enclosure for Protein?Ligand Complexes. *J. Med. Chem.* **2006,** *49* (21), 6177-6196.
8. Gordon, J. C.; Myers, J. B.; Timothy, F.; Valia, S.; Heath, L. S.; Alexey, O. J. N. A. R., H++: a server for estimating pKas and adding missing hydrogens to macromolecules. **2017,** *33* (Web Server issue), 368-371.
9. Duan, Y.; Wu, C.; Chowdhury, S.; Lee, M. C.; Xiong, G.; Zhang, W.; Yang, R.; Cieplak, P.; Luo, R.; Lee, T.; Caldwell, J.; Wang, J.; Kollman, P., A point-charge force field for molecular mechanics simulations of proteins based on condensed-phase quantum mechanical calculations. *J. Comput. Chem.* **2003,** *24* (16), 1999-2012.
10. Jorgensen, W. L.; Chandrasekhar, J.; Madura, J. D.; Impey, R. W.; Klein, M. L., Comparison of simple potential functions for simulating liquid water. *J. Chem. Phys.* **1983,** *79* (2), 926-935.
11. Wang, J.; Wolf, R. M.; Caldwell, J. W.; Kollman, P. A.; Case, D. A., Development and testing of a general amber force field. *J. Comput. Chem.* **2004,** *25* (9), 1157-1174.
12. Bayly, C. I.; Cieplak, P.; Cornell, W.; Kollman, P. A., A well-behaved electrostatic potential based method using charge restraints for deriving atomic charges: the RESP model. *J. Phys. Chem.* **1993,** *97* (40), 10269-10280.
13. Frisch, M. J. T., G. W.; Schlegel, H. B.; Scuseria, G. E.;; Robb, M. A. C., J. R.; Scalmani, G.; Barone, V.; Mennucci,; B.; Petersson, G. A. N., H.; Caricato, M.; Li, X.; Hratchian, H.; P.; Izmaylov, A. F. B., J.; Zheng, G.; Sonnenberg, J. L.; Hada, M.;; Ehara, M. T., K.; Fukuda, R.; Hasegawa, J.; Ishida, M.; Nakajima,; T.; Honda, Y. K., O.; Nakai, H.; Vreven, T.; Montgomery, J. A., Jr.;; Peralta, J. E. O., F.; Bearpark, M.; Heyd, J. J.; Brothers, E.; Kudin,; K. N.; Staroverov, V. N. K., R.; Normand, J.; Raghavachari, K.;; Rendell, A. B., J. C.; Iyengar, S. S.; Tomasi, J.; Cossi, M.; Rega,; N.; Millam, J. M. K., M.; Knox, J. E.; Cross, J. B.; Bakken, V.;; Adamo, C. J., J.; Gomperts, R.; Stratmann, R. E.; Yazyev, O.;; Austin, A. J. C., R.; Pomelli, C.; Ochterski, J. W.; Martin, R. L.;; Morokuma, K. Z., V. G.; Voth, G. A.; Salvador, P.;; Dannenberg, J. J. D., S.; Daniels, A. D.; Farkas, O..;; Foresman, J. B. O., J. V.; Cioslowski, J.; Fox, D. J., *Gaussian 09; Gaussian Inc., Wallingford, CT, 2009.*
14. Case, D. A. D., T. A.; Cheatham, T. E., III; Simmerling, C.; L.; Wang, J. D., R. E.; Luo, R.; Walker, R. C.; Zhang, W.; Merz, K.; M.; Roberts, B. H., S.; Roitberg, A.; Seabra, G.; Swails, J.; Goetz, A.; W.; Kolossvary, I. W., K. F.; Paesani, F.; Vanicek, J.; Wolf, R. M.;; Liu, J. W., X.; Brozell, S. R.; Steinbrecher, T.; Gohlke, H.; Cai, Q.; Ye,; X.; Wang, J. H., M. J.; Cui, G.; Roe, D. R.; Mathews, D. H.; Seetin,; M. G.; Salomon-Ferrer, R. S., C.; Babin, V.; Luchko, T.; Gusarov,; S.; Kovalenko, A. K., P. A., *AMBER12; University of California, San Francisco, CA, 2012.*
15. Ryckaert, J. P. C.; Ciccotti, G.; Berendsen, H. J. C., Numerical integration of the cartesian equations of motion of a system with constraints: molecular dynamics of n-alkanes. *J. Comput. Phys.* **1977,** *23*, 327-341.
16. Zhao, Y.; Truhlar, D. G., The M06 suite of density functionals for main group thermochemistry, thermochemical kinetics, noncovalent interactions, excited states, and transition elements: two new functionals and systematic testing of four M06-class functionals and 12 other functionals. *Theor. Chem. Acc.* **2008,** *120*,

215-241.
17. Zhao, Y.; Truhlar, D. G., Exploring the Limit of Accuracy of the Global Hybrid Meta Density Functional for Main-Group Thermochemistry, Kinetics, and Noncovalent Interactions. *J. Chem. Theory Comput.* **2008,** *4*, 1849-1868.
18. Chen, N.; Zhou, J.; Li, J.; Xu, J.; Wu, R., Concerted Cyclization of Lanosterol C-Ring and D-Ring Under Human Oxidosqualene Cyclase Catalysis: An ab Initio QM/MM MD Study. *J. Chem. Theory Comput.* **2014,** *10* (3), 1109-1120.
19. Chen, N.; Wang, S.; Smentek, L.; Hess, B. A., Jr.; Wu, R., Biosynthetic Mechanism of Lanosterol: Cyclization. *Angew. Chem. Int. Ed.* **2015,** *54* (30), 8693-8696.
20. Chu, Y.; Xu, Q.; Guo, H., Understanding Energetic Origins of Product Specificity of SET8 from QM/MM Free Energy Simulations: What Causes the Stop of Methyl Addition during Histone Lysine Methylation? *J. Chem. Theory Comput.* **2010,** *6* (4), 1380-1389.
21. Chu, Y.; Yao, J.; Guo, H., QM/MM MD and Free Energy Simulations of G9a-Like Protein (GLP) and Its Mutants: Understanding the Factors that Determine the Product Specificity. *Plos One* **2012,** *7* (5), e37674.
22. Hu, P.; Wang, S.; Zhang, Y., How Do SET-Domain Protein Lysine Methyltransferases Achieve the Methylation State Specificity? Revisited by Ab Initio QM/MM Molecular Dynamics Simulations. *J. Am. Chem. Soc.* **2008,** *130* (12), 3806-3813.
23. Zhou, Y.; Wang, S.; Li, Y.; Zhang, Y., Born-Oppenheimer Ab Initio QM/MM Molecular Dynamics Simulations of Enzyme Reactions. *Methods Enzymol.* **2016,** *577*, 105-118.
24. Zhang, Y.; Liu, H.; Yang, W., Free energy calculation on enzyme reactions with an efficient iterative procedure to determine minimum energy paths on a combined ab initio QM/MM potential energy surface. *J. Chem. Phys.* **2000,** *112*, 3483-3492.
25. Torrie, G. M.; Valleau, J. P., Nonphysical sampling distributions in Monte Carlo free-energy estimation: Umbrella sampling. *J. Comput. Phys.* **1977,** *23*, 187-199.
26. Kumar, S.; Rosenberg, J. M.; Bouzida, D.; Swendsen, R. H.; Kollman, P. A., THE weighted histogram analysis method for free-energy calculations on biomolecules. I. The method. *J. Comput. Chem.* **1992,** *13*, 1011-1021.
27. Souaille, M.; Roux, B. T., Extension to the weighted histogram analysis method: combining umbrella sampling with free energy calculations. *Comput. Phys. Commun.* **2001,** *135*, 40-57.
28. Shao, Y.; Fusti-Molnar, L. J., Y.; Kussmann, J.; Ochsenfeld C.; Brown, S. T.; Gilbert, A. T.; Slipchenko, L. V.; Levchenko, S. V.; O'Neill, D. P.; DiStasio, R. A.; Lochan, R. C.; Wang, T.; Beran, G. J.; Besley, N. A.; Herbert, J. M.; Lin, C. Y.; Van Voorhis, T.; Chien, S. H.; Sodt, A.; Steele, R. P.; Rassolov, V. A.; Maslen, P. E.; Korambath, P. P.; Adamson, R. D.; Austin, B.; Baker, J.; Byrd, E. F.; Dachsel, H.; Doerksen, R. J.; Dreuw, A.; Dunietz, B. D.; Dutoi, A. D.; Furlani, T. R.; Gwaltney, S. R.; Heyden, A.; Hirata, S.; Hsu, C. P.; Kedziora, G.; Khalliulin, R. Z.; Klunzinger, P.; Lee, A. M.; Lee, M. S.; Liang, W.; Lotan, I.; Nair, N.; Peters, B.; Proynov, E. I.; Pieniazek, P. A.; Rhee, Y. M.; Ritchie, J.; Rosta, E.; Sherrill, C. D.; Simmonett, A. C.; Subotnik, J. E.; Woodcock, H. L.; Zhang, W.; Bell, A. T.; Chakraborty, A. K.; Chipman, D. M.; Keil, F. J.; Warshel, A.; Hehre, W. J.; Schaefer, H. F.; Kong, J.; Krylov, A. I.; Gill, P. M.; Head-Gordon, M. , Advances in methods and algorithms in a modern quantum chemistry program package. *Phys. Chem. Chem. Phys.* **2006,** *8*, 3172-3191.

V. NMR spectra

^{1}H NMR (500 MHz, $CDCl_3$) of compound **18**

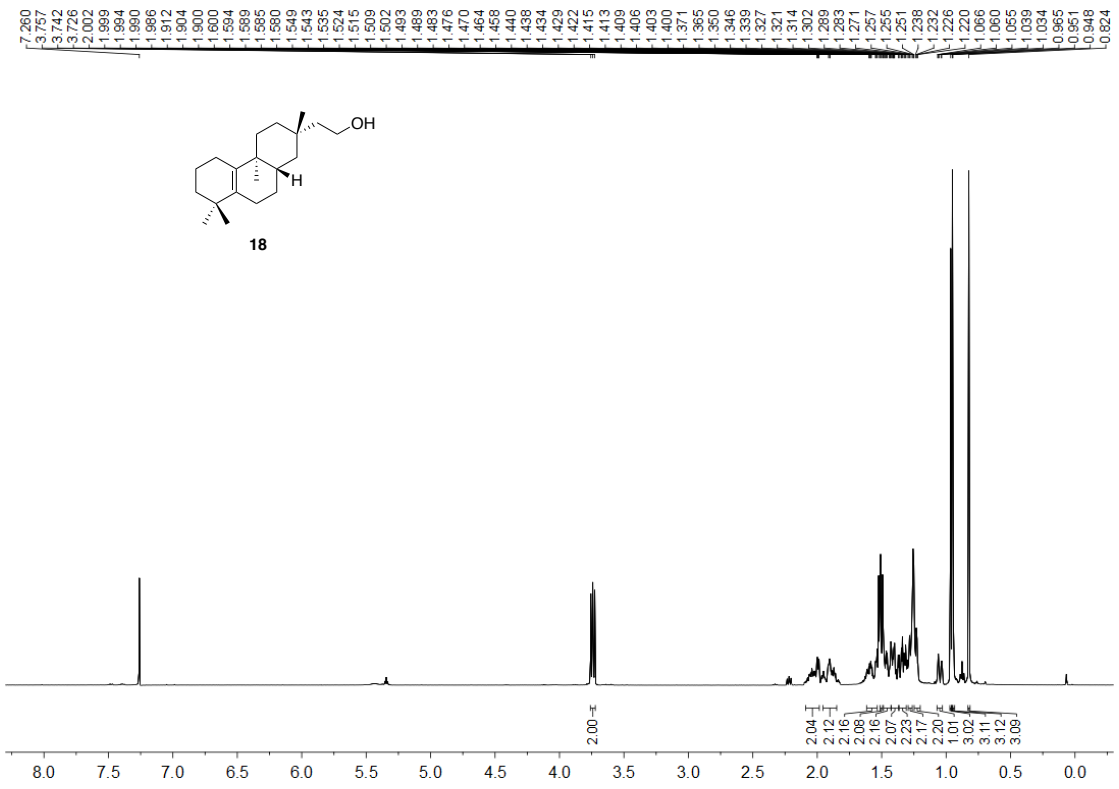

^{13}C NMR (126 MHz, $CDCl_3$) of compound **18**

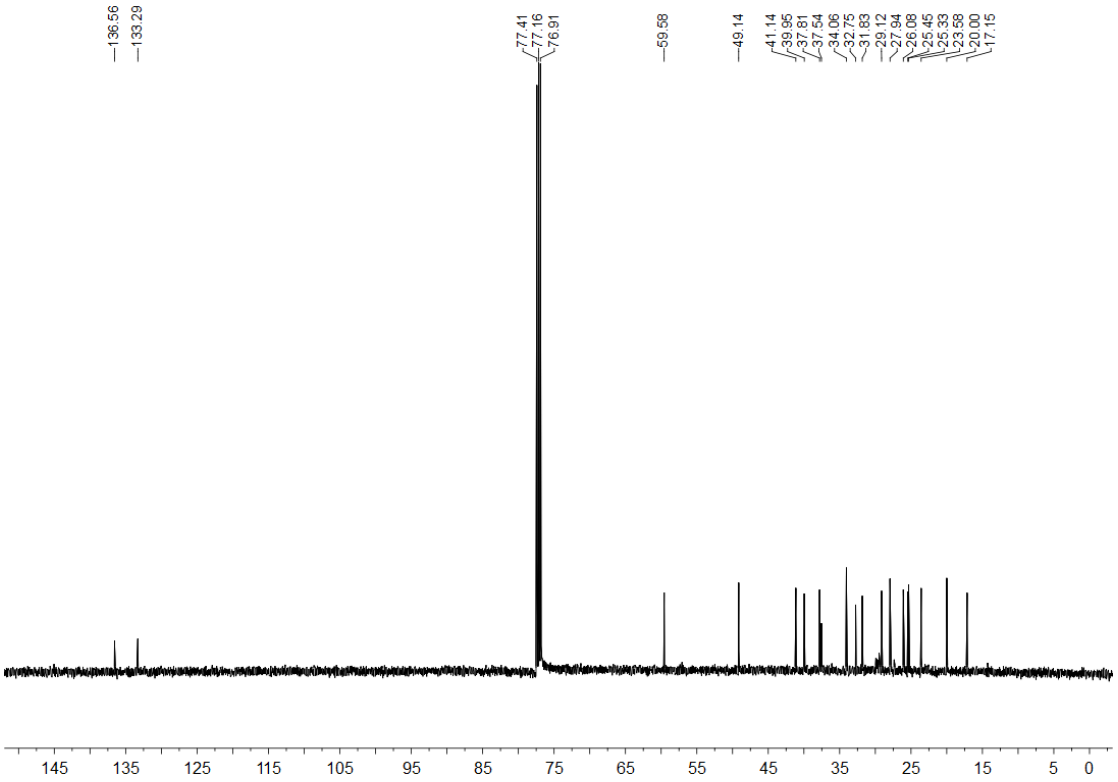

DEPT of compound **18**

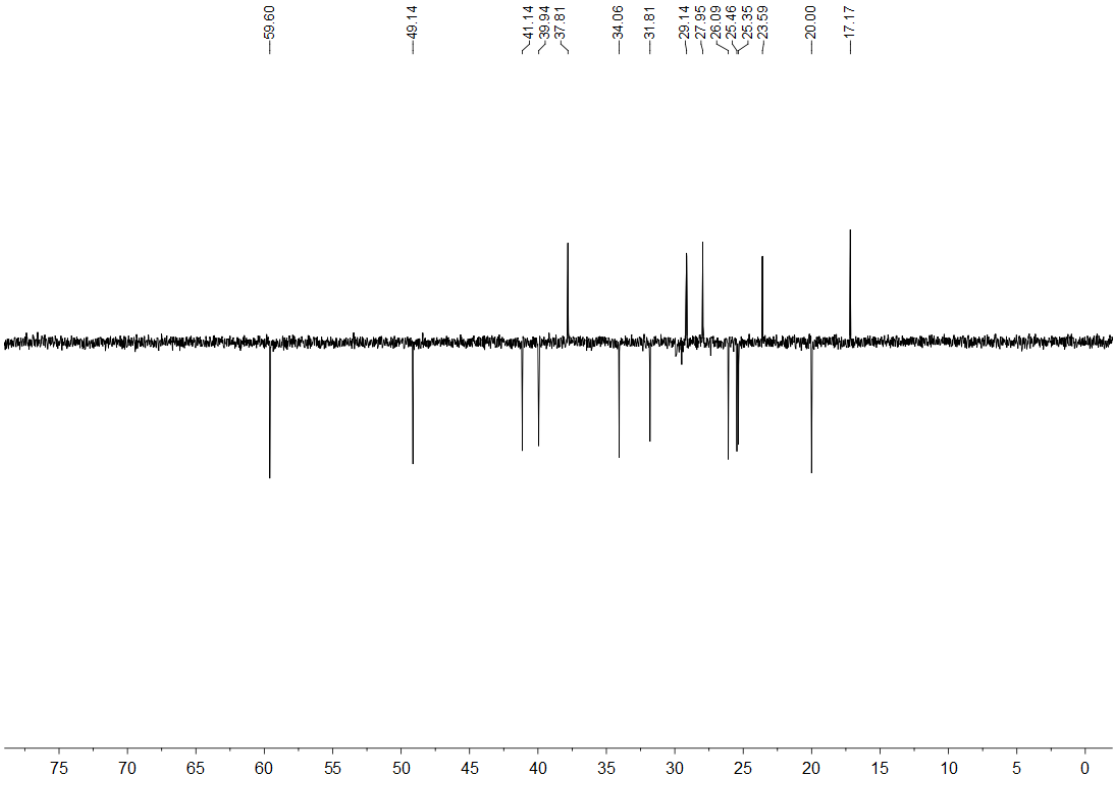

COSY of compound **18**

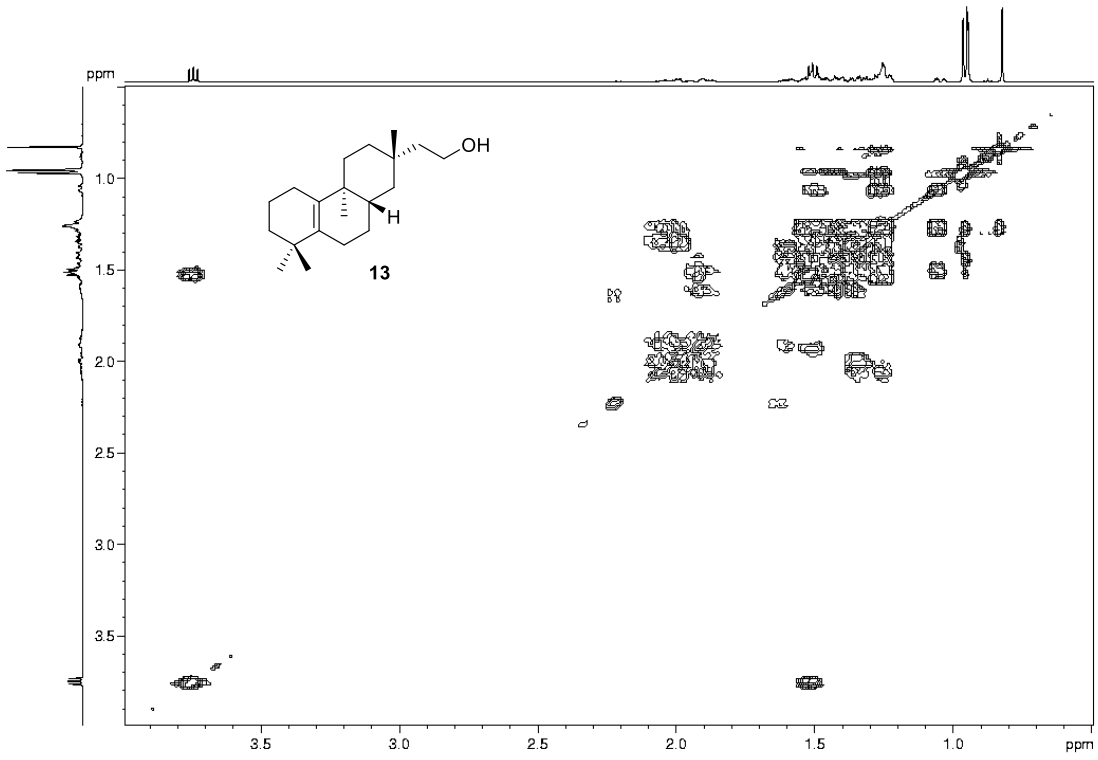

HMBC of compound **18**

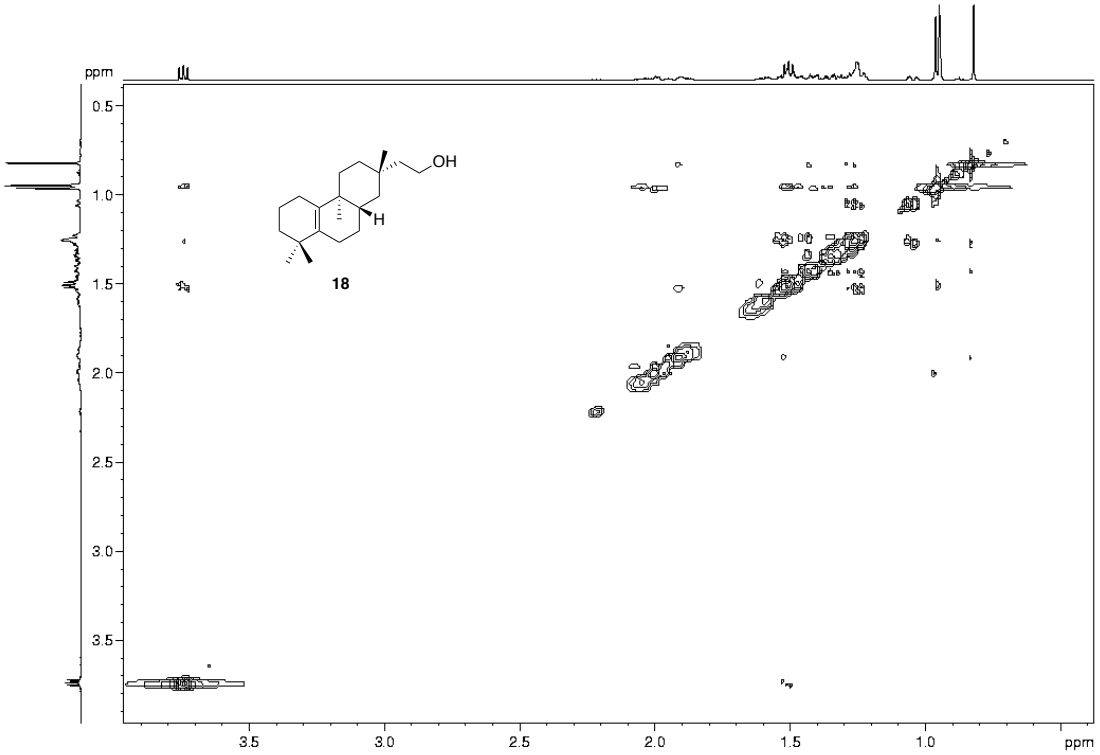

HMBC of compound **18**

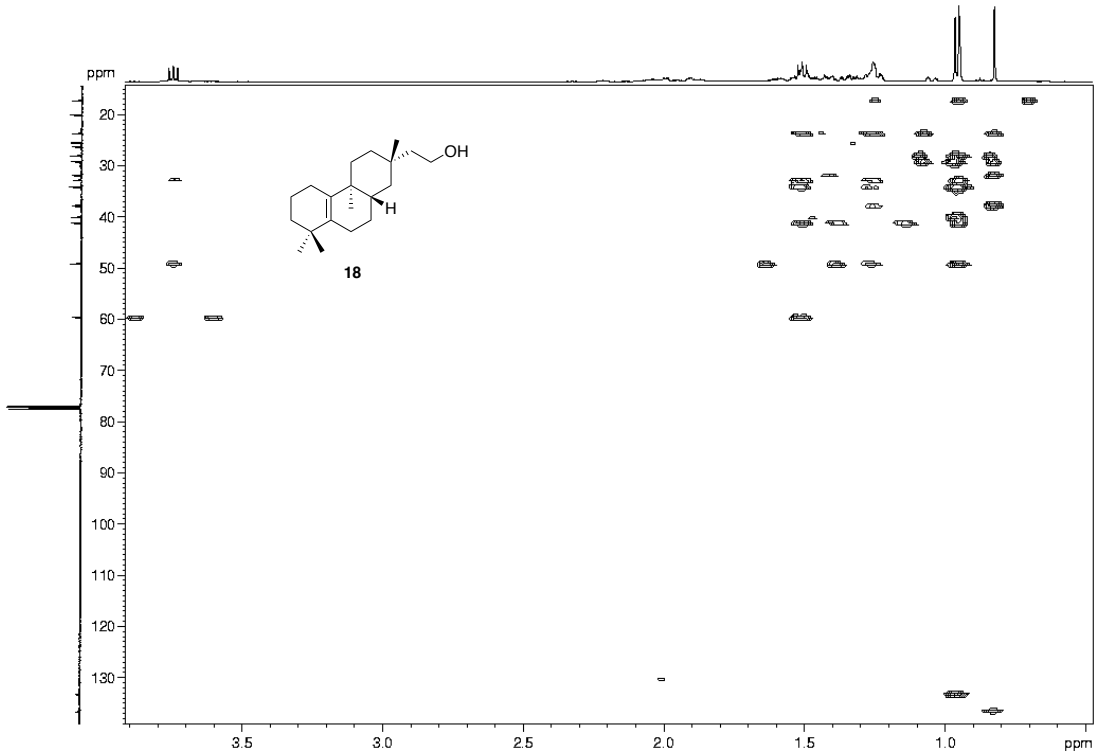

HSQC of compound **18**

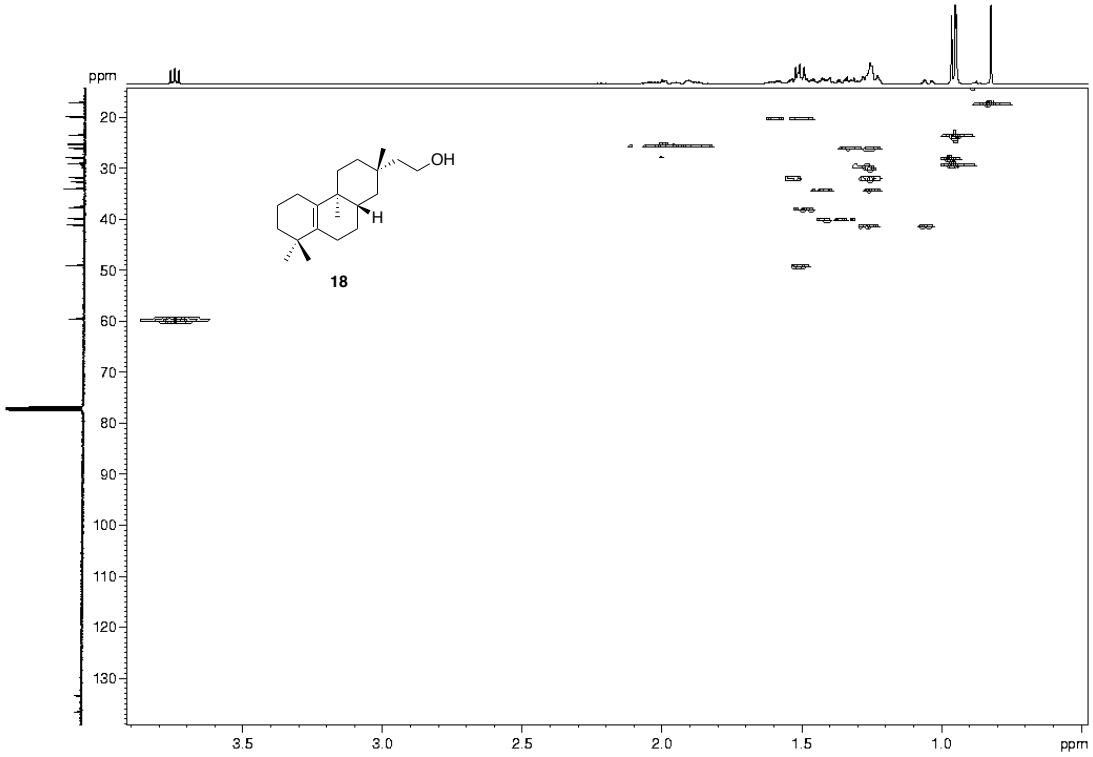

^{1}H NMR (500 MHz, $CDCl_3$) of compound **19**

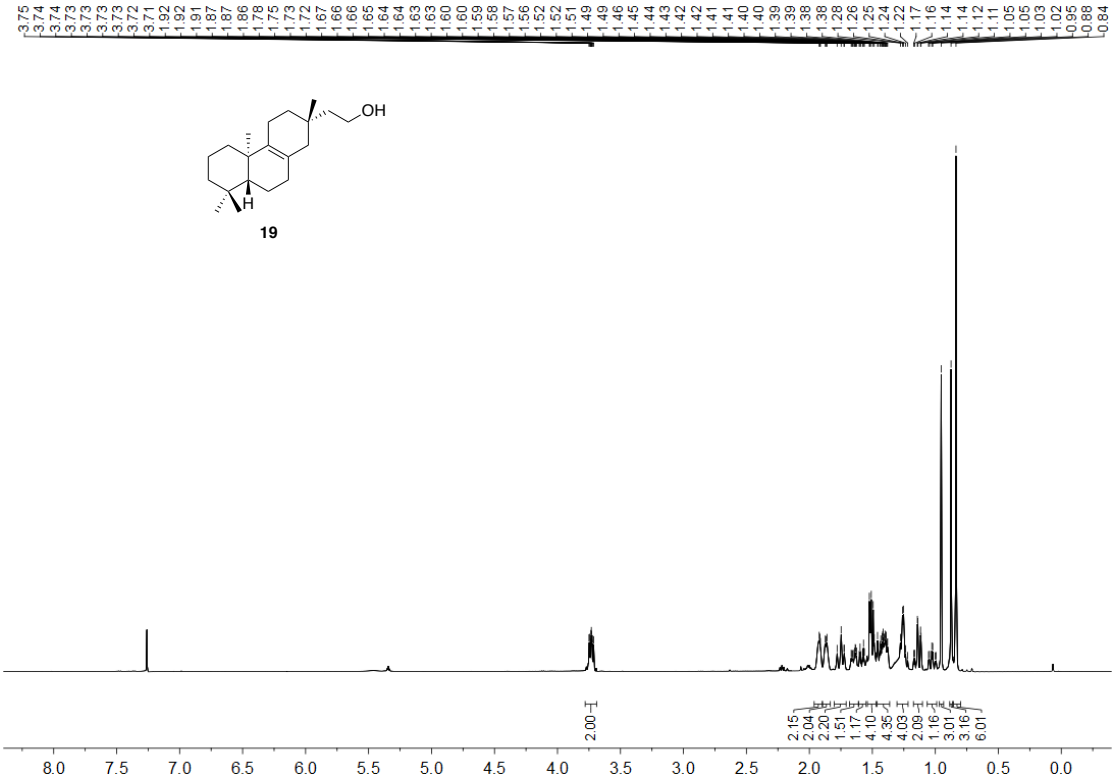

^{13}C NMR (126 MHz, $CDCl_3$) of compound **19**

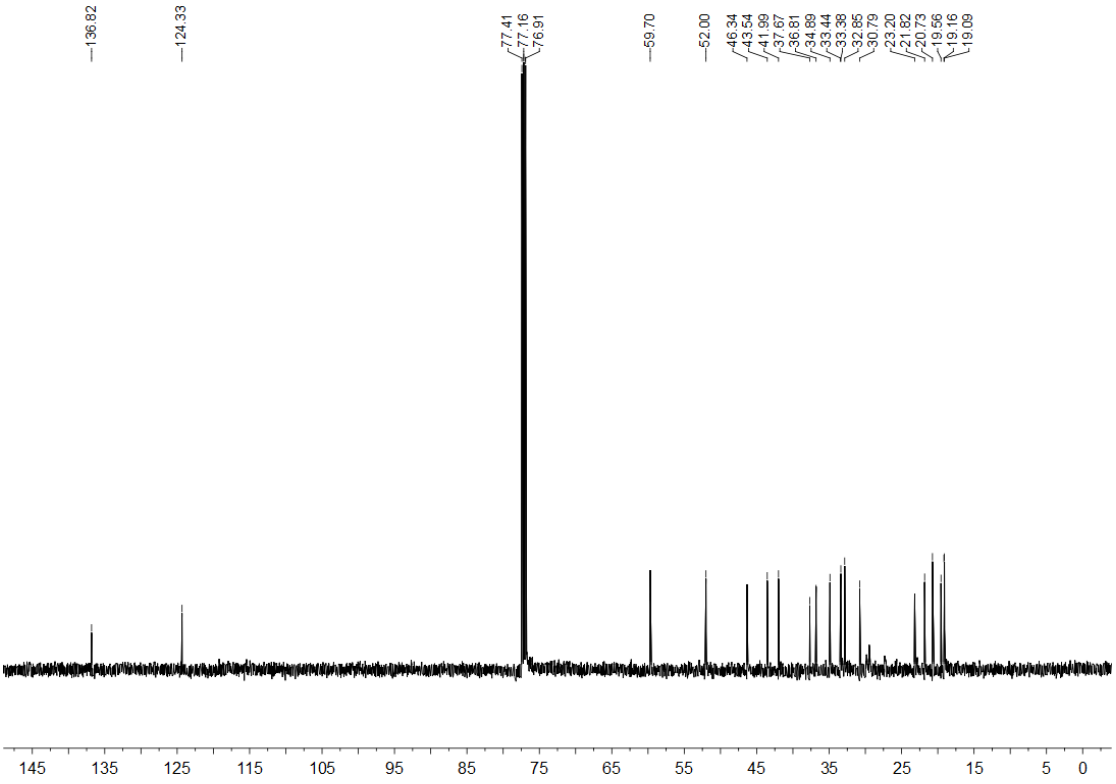

DEPT of compound **19**

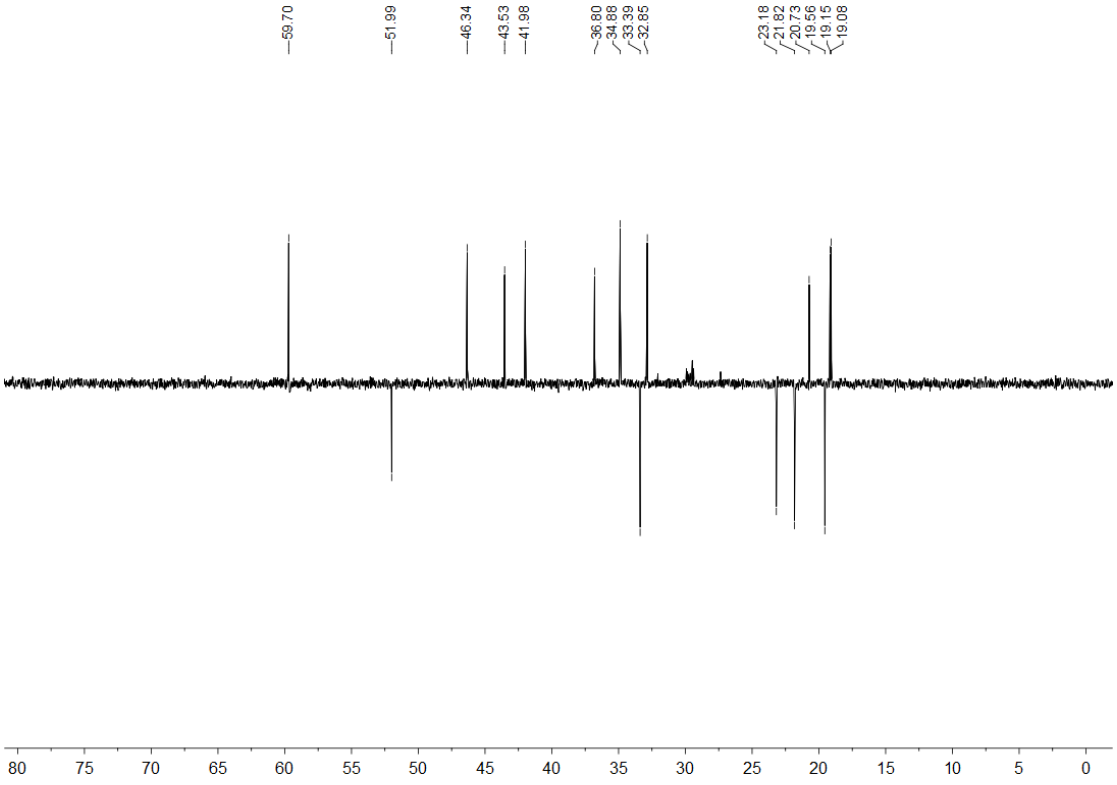

COSY of compound **19**

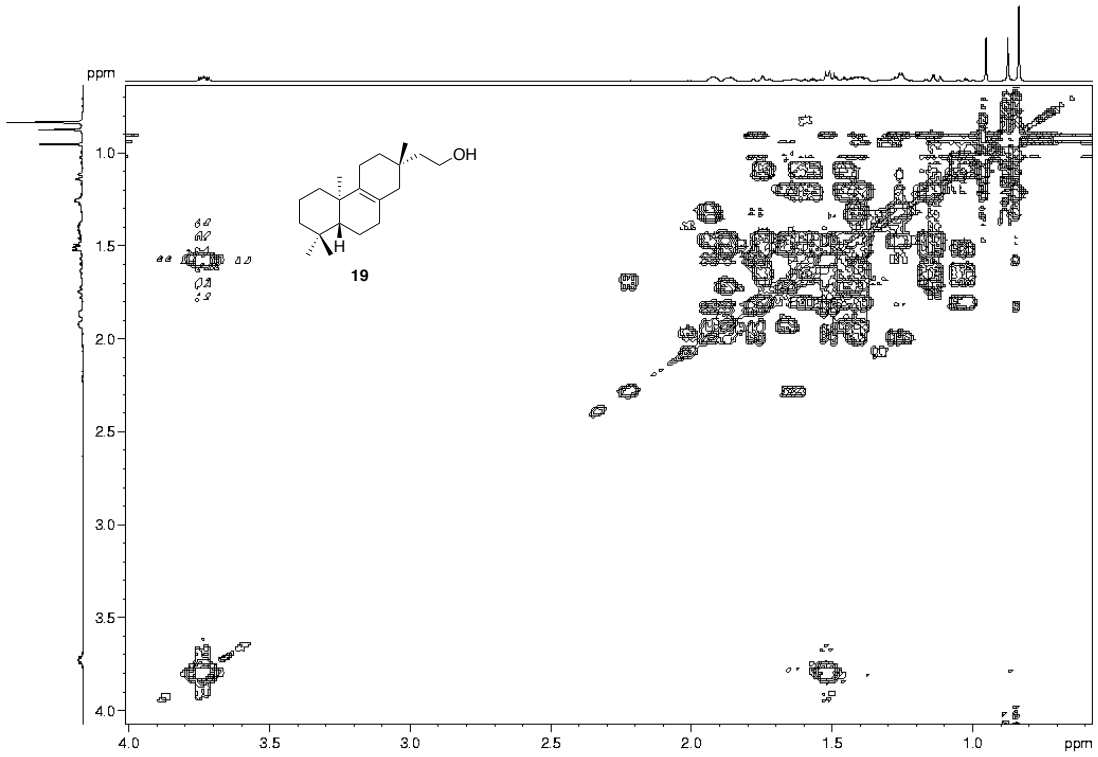

NOESY of compound **19**

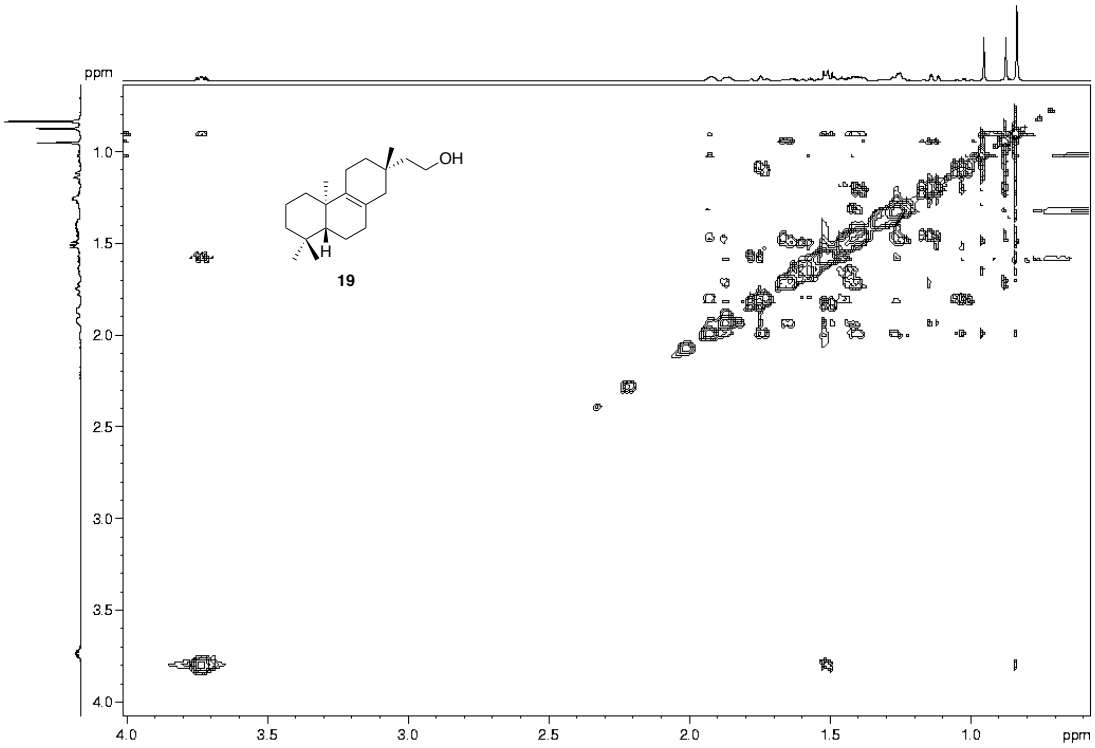

HMBC of compound **19**

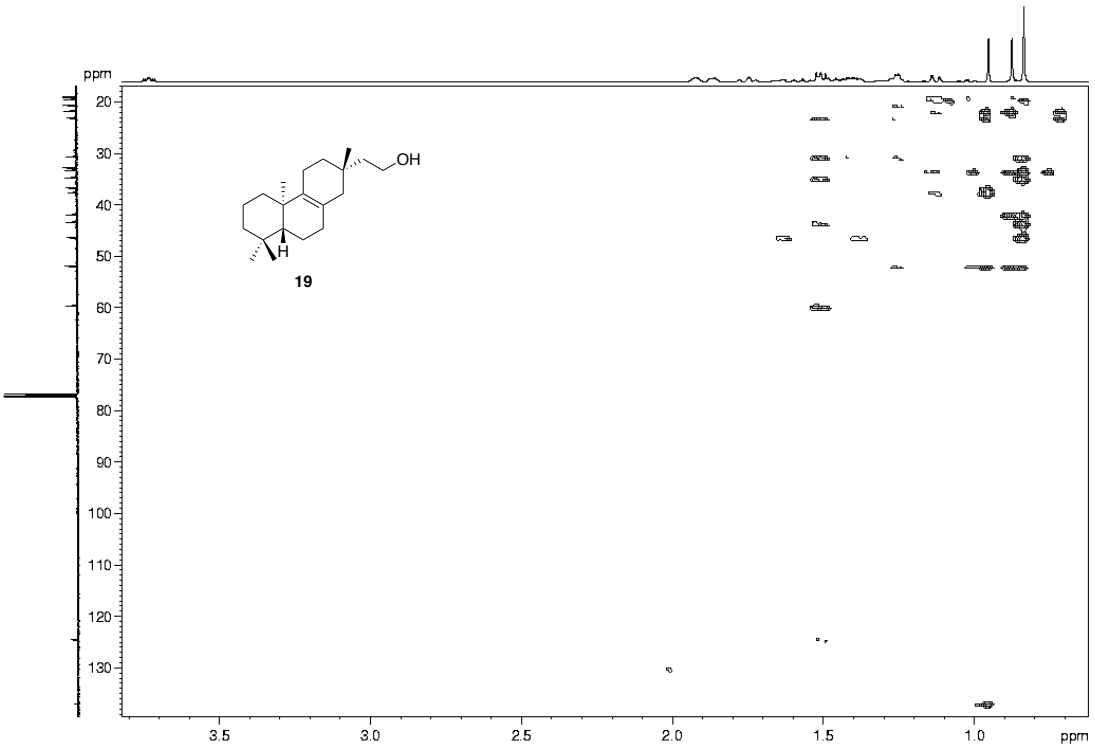

HSQC of compound **19**

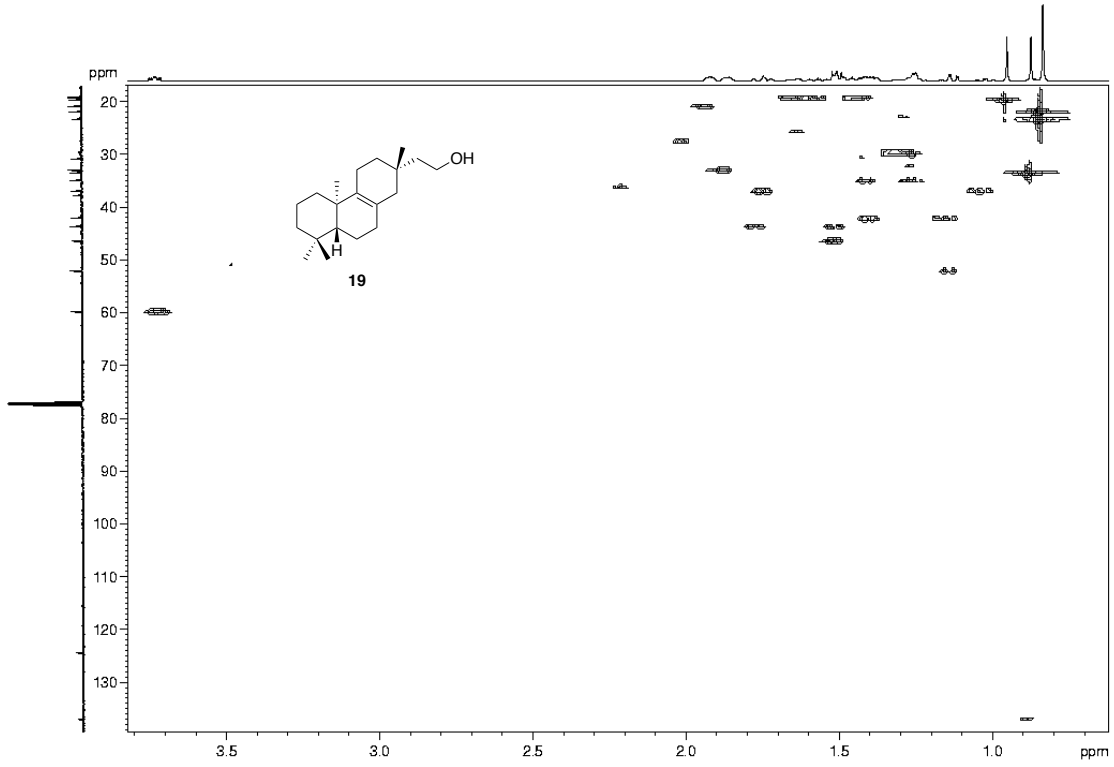

^{1}H NMR (500 MHz, $CDCl_3$) of compound **10**

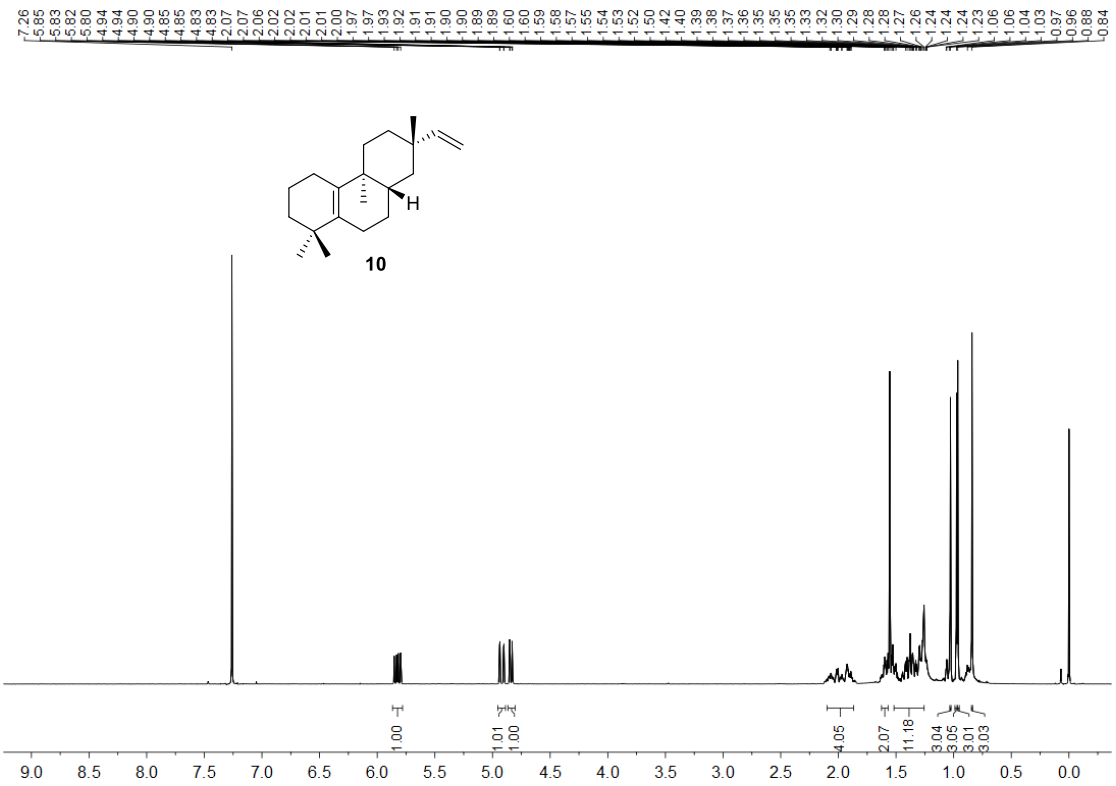

^{13}C NMR (126 MHz, $CDCl_3$) of compound **10**

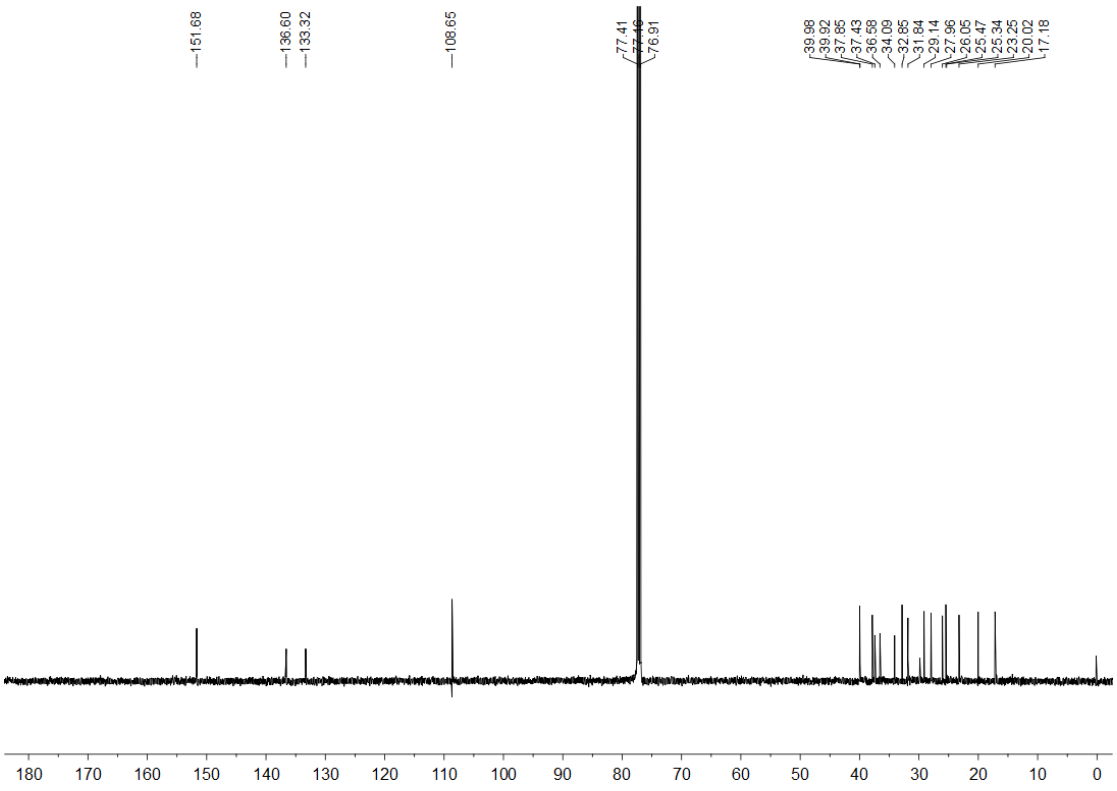

^{1}H NMR (500 MHz, $CDCl_3$) of compound **S1**

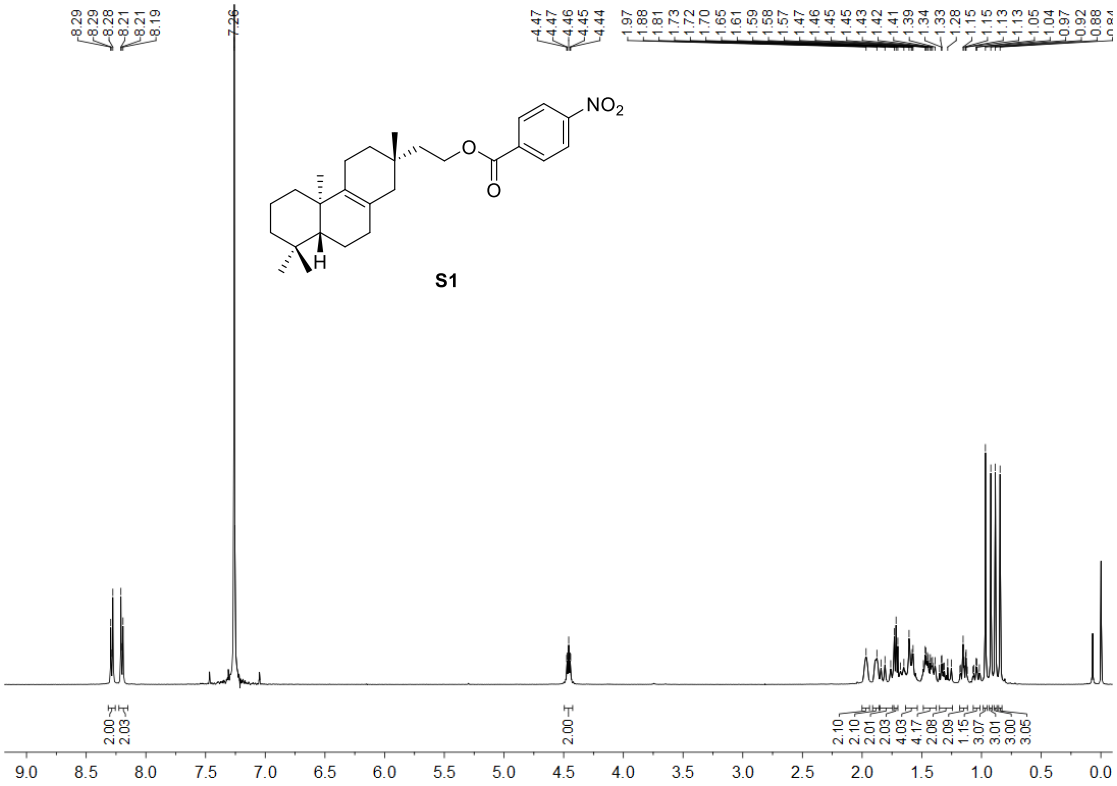

^{13}C NMR (126 MHz, $CDCl_3$) of compound **S1**